Coordination Chemistry Reviews 255 (2011) 1268–1292

Contents lists available at ScienceDirect

Coordination Chemistry Reviews

journal homepage: www.elsevier.com/locate/ccr

Review

Advances in alkaline earth-nitrogen chemistry

Ana Torvisco[a], Anna Y. O'Brien[b], Karin Ruhlandt-Senge[a,*]

[a] Deparment of Chemistry, CST 1-014, Syracuse University, Syracuse, NY 13244, USA
[b] Department of Chemistry and Physics, 1419 Salt Springs Road, Le Moyne College, Syracuse, NY 13214, USA

Contents

Abbreviations: Ae, magnesium, calcium, strontium, barium; CN, coordination number; THF, thf, tetrahydrofuran; HEX, hex, hexane; HMPA, hmpa, hexamethylphosphoric acid triamide; $OPPh_3$, triphenylphosphane oxide; PMDTA, pmdta, *N*, *N*, *N*′, *N*′, *N*″-pentamethyldiethylenetriamine; TMEDA, tmeda, *N*, *N*, *N*′, *N*′-tetramethylethylenediamine; $H_2N(Ph)$, aniline; $H_2N(Mes)$, 2,4,6-trimethylaniline; $H_2N(Dipp)$, 2,6-di-isopropylaniline; $H_2N(Mes^*)$, 2,4,6-tri-*tert*-butylaniline; $HN(SiMe_3)_2$, 1,1,1,3,3,3-hexamethyldisilazane, HMDS; $HN(Ph)(SiMe_3)$, *N*-(trimethylsilyl)aniline; $HN(Mes)(SiMe_3)$, 2,4,6-trimethyl-*N*-(trimethylsilyl)aniline; $HN(Dipp)(SiMe_3)$, 2,6-di-isopropyl-*N*-(trimethylsilyl)aniline; $HN(SiMePh_2)_2$, bis(bisdiphenylmethylsilylamine); BDI, β-diketiminate; Pz, pyrazolate; Bp, dihydrobis(pyrazolyl)borate; Tp, hydrotris(pyrazolyl)borate.

* Corresponding author. Tel.: +1 315 443 1306; fax: +1 315 443 4070.
E-mail address: kruhland@syr.edu (K. Ruhlandt-Senge).

0010-8545/$ – see front matter
doi:10.1016/j.ccr.2011.02.015

ARTICLE INFO

Article history:
Received 9 January 2011
Accepted 19 February 2011
Available online 1 March 2011

Keywords:
Alkaline earth
Nitrogen-based ligands
Amides
Secondary interactions
Coordination compounds
Pyrazolates
Tris(pyrazolyl)borate

ABSTRACT

This article provides a concise summary of alkaline earth metal nitrogen chemistry. This important area of s-block metal chemistry is shedding important light on the recent development of alkaline earth metal chemistry, as the preparation of the target compounds utilizes a large variety of synthetic methodology. Further, the compounds have been utilized in a range of applications, including polymerization initiation, catalysis, as solid-state precursors, and even high energy materials.

1. Introduction

1.1. Alkaline earth metals

The chemistry of the heavy alkaline earth metals (Ca, Sr, Ba) has progressed rapidly in recent years due to improved synthetic methodologies and renewed interest in applications ranging from materials to polymer chemistry. These developments are significant given the challenge of working with these metals. Their high tendency towards hydrolysis requires careful measures to avoid forming the more stable oxygen containing compounds. Among the alkaline earth metals, magnesium has been the most intensely studied, rationalized by the importance of magnesium amides in synthetic applications [1,2]. In contrast, the exploration of the heavy congeners has been marred by synthetic challenges related to their: (i) higher oxo- and hydrophilicity, (ii) the larger metal centers and the resulting tendency towards aggregation and consequent solubility challenges, and (iii) the largely electrostatic metal–ligand interactions that render the coordination chemistry of the metal strongly ligand and co-ligand dependent [1–3]. Much progress has been made in understanding and addressing these challenges through the work done on alkaline earth metal compounds containing nitrogen-based ligands.

1.2. Factors affecting alkaline earth metal compound stability

Atomic radii increase down a group and decrease across a row, making the heavy s-block metals the largest in the Periodic Table [3]. As a result, metal aggregation is frequently observed for Ca, Sr, and Ba, leading to high coordination numbers and subsequently poor compound solubility [2]. In addition, the weak metal–ligand bonds typically result in compounds with significant lability. These factors lead to the facile formation of oxides and hydroxides in the presence of air or water. Strategies for stabilizing alkaline earth metal compounds have focused on saturating the metal coordination spheres and tailoring ligand systems to suit the specific metal–ligand bond characteristic.

Metal–ligand bond characteristics are critically influenced by the metal charge/size ratio. The lighter metals, beryllium and magnesium, with their smaller diameters, display relatively high charge/size ratios compared to calcium, strontium and barium. High charge/size ratios coincide with the capacity for bond polarization and the induction of bond covalency. As such, among the alkaline earth metals, beryllium and magnesium display metal–nitrogen bonds with the highest covalent character. Nonetheless, differences in the electronegativities of the metal and nitrogen impart significant polar character to the respective bonds [1–5].

Due to their increased covalent character, beryllium and magnesium amides, for example, typically display a preference for contact molecules, although the utility of beryllium amides is hampered by the toxic nature of the metal [6]. As the charge/size ratio decreases for the larger metals, the metal–ligand bonds become weaker and ion dissociation is expected to become more prevalent. The three ion dissociation modes for alkaline earth metals are shown in Scheme 1. Investigations of ligand systems that result in the formation of dissociated ions will lead to further understanding of the metal–ligand characteristics of the heavier alkaline earth metals.

The typical strategy for stabilizing compounds of the heavier alkaline earth metals has been the use of sterically demanding ligands, allowing the isolation of a range of nitrogen-based species [7–12]. In instances when ligand bulk is not sufficient to affect metal stabilization, steric saturation has been achieved by the coordination of neutral donors, circumventing oligomerization and increasing solubility. Studies delineating donor effects on compound stability and structure/function relationships have been instrumental in further understanding the coordination chemistry of these large metals [2].

The presence of secondary non-covalent interactions is not insignificant when considering factors that stabilize these compounds. In reviewing the large number of alkaline earth nitrogen-based compounds, it is apparent that non-covalent interactions in the form of M···C(π) interactions and M···H–C agostic interactions are an important means to provide further steric saturation of the large alkaline earth metal centers. Although these are significantly weaker than covalent interactions, in light of the weak alkaline earth metal–ligand bonds, they play a significant role

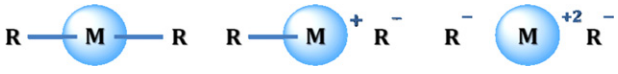

Scheme 1. Ion-association modes for alkaline earth metals.

in metal stabilization; especially since multiple weak interactions are frequently observed.

Metal···C(π) interactions are a prevalent stabilizing force in alkaline earth metal chemistry [13–16], as summarized in Table 1. However, less is known about the role that agostic interactions of the type M···H–C play in stabilizing these metal centers. Agostic interactions are described as weak interactions of a coordinatively unsaturated metal with a C–H bond [17–19]. Although present in a large number of alkaline earth compounds, agostic interactions are rarely reported and frequently ignored, despite their prevalence and growing importance in the steric and electronic stabilization of large, highly reactive metal centers [18,19].

Perhaps the lack of acknowledgment of agostic interactions can be partially attributed to difficulties in locating hydrogen positions in crystallographic experiments. In order to circumvent locating these interactions, they are often reported as M···C interactions. Further complicating the identification of these weak interactions is that formal cut-off values have not been well established. All agostic interactions reported herein are within range of the sum of van der Waals radii ($\Sigma(r_{wAe} + r_{wH})$) for a metal–hydrogen bond, and are summarized in Table 2 [4], along with cut-off values established from published work [18,19].

The importance of stabilizing factors such as non-covalent interactions and their overall effect on ion-association, geometry, and resulting structure/function relationships will be highlighted throughout this article.

2. Alkaline earth amides

The chemistry of the alkaline earth metal amides has progressed significantly in the last 50 years due to advances in their synthetic methodology and in the understanding of the role ligands and co-ligands play in stabilizing the compounds and ensuring solubility. The implications on synthesis, reactivity, and geometry will be discussed as we study the effects of steric saturation of the metal center as achieved by ligand bulk and effects of varying substitution patterns.

2.1. Secondary silylated amines

The bis(trimethylsilyl)amine, $HN(SiMe_3)_2$, often referred to as HMDS, ligand has truly been the cornerstone of alkaline earth amido chemistry, and through the study of this ligand, a greater understanding of the synthesis and structure/function relationship of early main group compounds has been possible. This sterically encumbering ligand has been used extensively to afford stable, soluble compounds with low metal coordination numbers, including donor-free dimers [20–23], in addition to donor-containing monomers [23–25]. Bis(trimethylsilyl)amine derivatives for the heavier alkaline earth congeners may be accessed by transmetallation reaction with tin or mercury bis(bis(trimethylsilyl)amide) with alkaline earth metals in toluene (Scheme 2, Route iv) [20,21,23,25,26]. Alternatively, organoelimination for magnesium (Scheme 2, Route vi) [22,27,28], salt metathesis (Scheme 2, Route i) [29], and direct metallation through ammonia activation (Scheme 2, Route ii) [23,30] have been examined. Recent advances include the use of the benign $BiPh_3$ in redox transmetallation/ligand exchange (RTLE) offering the amides in excellent yields and purity in a simple procedure (Scheme 2, Route v) [16,19].

Aside from allowing the isolation of compounds exhibiting low metal nuclearity and coordination numbers, amides based on the bis(trimethylsilyl)amine ligand exhibit excellent solubility in both polar and non-polar solvents. These amides are also excellent starting materials towards a range of alkaline earth metal compounds due to its relatively high pK_a of 25.8 (DMSO) [31] allowing

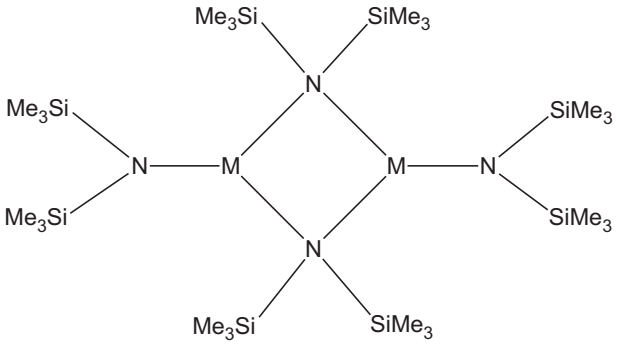

Fig. 1. The alkaline earth metal M_2N_4 core in $[M\{N(SiMe_3)_2\}_2]_2$ dimers.

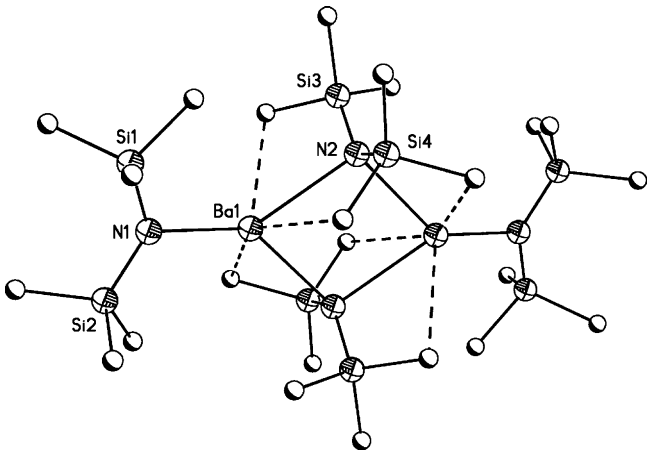

Fig. 2. Structure of $[Ba\{N(SiMe_3)_2\}_2]_2$ [23]. Hydrogen atoms removed for clarity. Agostic interactions shown as dashed lines.

the preparation of other synthetic targets (Scheme 2, Route viii) [2,7].

In the case of the smallest alkaline earth metal, beryllium, the $[N(SiMe_3)_2]^-$ ligand is sufficiently bulky to allow the formation of a monomeric $Be[N(SiMe_3)_2]_2$ [32–34]. However, for the larger alkaline earth metals, in the absence of co-ligands, dimeric species of the form $[M\{N(SiMe_3)_2\}_2]_2$ are observed. In fact, all HMDS based alkaline earth metal amides, except the beryllium species, dimerize (Fig. 1) in the solid state in an isostructural M_2N_4 motif [20–23]. These compounds have been reviewed previously and will not be considered here [7].

Despite the increase in metal ionic radii descending down the group (Mg = 0.72, Ba = 1.35 Å; CN = 6) [3] each metal displays a low coordination number due to the inherent kinetic stabilization which the $[N(SiMe_3)_2]^-$ ligand affords to the metal centers. Upon closer inspection, a second factor in allowing the isolation of these stable low coordinate species lies in the presence of agostic interactions arising from the trimethylsilyl substituents. Due to inherent difficulties in locating hydrogen atoms, these interactions were reported as M···C interactions. These values and extrapolated M···H–C agostic interactions are summarized in Table 3 (Fig. 2).

The dynamic behavior of the silylated secondary amides in solution was analyzed using VT NMR studies, with the free energy of activation $\Delta G^{\ddagger}$ for the dynamic exchange of the $[N(SiMe_3)_2]^-$ ligands determined to be 17.20 and 12.67 kcal/mol for the Ca and Sr compounds [26]. The smaller value for the heavier analogue is indicative of the reduced metal–ligand bond strength.

For compounds containing the $[N(SiMe_3)_2]^-$ ligand, the use of neutral donors has been effective in isolating compounds with reduced nuclearity. This has been achieved either by the synthesis of these compounds in ethereal solutions (tetrahydrofuran

Table 1
van der Waals radii and M···C(π) interaction cut-off values for alkaline earth metals.

M^{2+}	CN	r_{ion} [3]	r_w [4] (C = 1.70) (Å)	$\Sigma(r_{wM} + r_{wH})$ (M–C) (Å)	Cut-off value[a] (M···C(π)) (Å)	Experimental range (Å) [14,16,13]
Mg	6	0.72	1.73	3.43		
Ca	6	1.00	2.31	4.01	3.20	2.84–3.13
Sr	6	1.18	2.49	4.19	3.35	3.02–3.30
Ba	6	1.35	2.68	4.38	3.50	3.13–3.48

[a] Cut-off values used in this work.

Table 2
van der Waals radii and M···H–C agostic interaction cut-off values for alkaline earth metals.

M^{2+}	CN	r_{ion} [3]	r_w [4] (H = 1.10) (Å)	$\Sigma(r_{wM} + r_{wH})$ (M–H) (Å)	Cut-off value[a] (M···H–C) (Å)	Experimental range [18,19] (Å)
Mg	6	0.72	1.73	2.83	2.50	1.99–2.49
Ca	6	1.00	2.31	3.41	3.10	2.68–3.05
Sr	6	1.18	2.49	3.59	3.25	2.83–3.19
Ba	6	1.35	2.68	3.78	3.30	2.84–3.23

[a] Cut-off values used in this work.

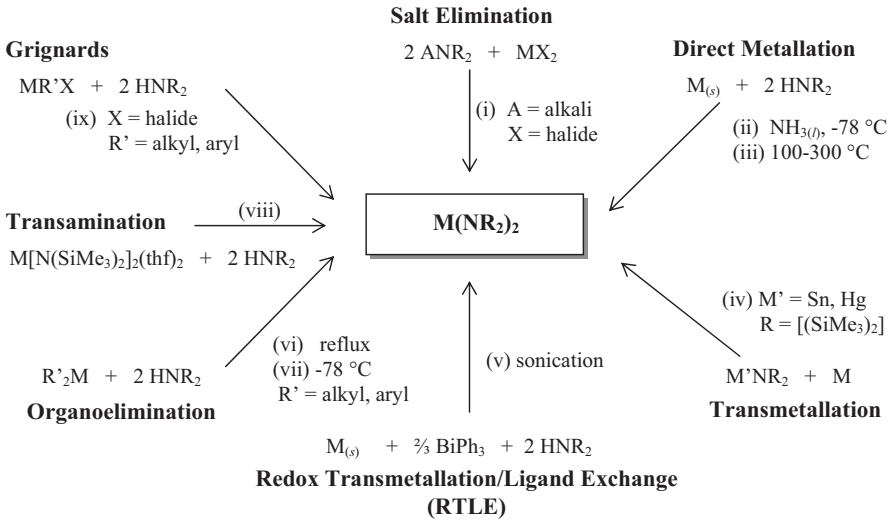

Scheme 2. Reaction routes towards alkaline earth metal species.

Table 3
Reported secondary interactions for $[M\{N(SiMe_3)_2\}_2]_2$.

	CN	M···C (Å)	M···H–C (Å) [18]	References
$[Ca\{N(SiMe_3)_2\}_2]_2$	3 + 4	2.827(10)–3.068(9)	2.339–2.829	[20]
$[Sr\{N(SiMe_3)_2\}_2]_2$	3 + 4	3.00(2)–3.18(2)	2.454–3.183	[21]
$[Ba\{N(SiMe_3)_2\}_2]_2$	3 + 6	3.169–3.342	2.320–3.226	[18]

(THF), or 1,2-dimethoxyethane (DME)) resulting in monomeric four coordinate species $M[N(SiMe_3)_2]_2(donor)_x$ (donor = THF, $x = 2$, M = Mg–Ba; donor = DME, $x = 1$, M = Ca, Sr) where the THF adducts are further stabilized by secondary interactions (Table 4) [20,21,25]. Donor exchange reactions with Lewis bases (pyridine (pyr), 1,4-dioxane) [20,21,24,25,35–39] allowed for the isolation of dimeric $\{[Mg[N(SiMe_3)_2]_2]_2(dioxane)\}$ [35] and the polymeric $\{Sr[N(SiMe_3)_2]_2(dioxane)\}_\infty$ [36,37]. Aggregation of the strontium species is attributed to its higher ionic radii and subsequent higher need for steric saturation as compared to magnesium. This is also evident by a close M···C interaction (3.16 Å) between the strontium metal center and a trimethylsilyl group (Table 4) [36,37]. DME as a solvent leads to the corresponding adducts for Ca and Sr, $M[N(SiMe_3)_2]_2(dme)$ whereas pyridine and TMEDA (Tetramethylethylenediamine) adducts for calcium were only verified by ^1H NMR studies [25]. Likewise use of $OPPh_3$, allows the isolation of the four-coordinate, $Ca[N(SiMe_3)_2]_2(OPPh_3)_2$ [40]. Similarly, in the case of barium, the larger ionic radii of the metal center, allows for the coordination of THF molecules to the metal center in the dimeric species $[\{Ba[N(SiMe_3)_2]_2(thf)\}_2]$ [23].

Table 4
Reported secondary interactions for $M[N(SiMe_3)_2]_2(donor)_x$.

	CN	M···H–C (Å)	M···C (Å)	References
$Ca[N(SiMe_3)_2]_2(thf)_2$	4 + 3	2.792–2.866		
$Sr[N(SiMe_3)_2]_2(thf)_2$	4 + 6	2.861–3.144		[18]
$Ba[N(SiMe_3)_2]_2(thf)_2$	4 + 8	3.056–3.197		
$\{Sr[N(SiMe_3)_2]_2(dioxane)\}_\infty$	4 + 1		3.16	[36,37]

Treatment of $Mg[N(SiMe_3)_2]_2(thf)_2$ with two equivalents of pyridine, 2,3,5-collidine, 4-picoline, or 3,5-lutidine led to the corresponding four coordinate species, $Mg[N(SiMe_3)_2]_2(pyr^*)_2$ [41,42]. However when the sterically more demanding co-ligands 2-picoline and 2,6-lutidine were used, monomeric three coordinate species, $Mg[N(SiMe_3)_2]_2(pyr^*)$, were obtained. In both cases, the sum of the angles about magnesium was 359.5°, indicating nearly perfect planarity, and the donors were perpendicular to the plane of the ligand.

Fewer bis(bis(trimethylsilyl)amide) donor adducts are known for the heavier alkaline earth metals, possibly due to their higher reactivity and higher lability of the M–N bond. Reaction of solvent free alkaline earth metal amides $[M\{N(SiMe_3)_2\}_2]$ with either 1,3-bis(2,4,6-trimethylphenyl)imidazolium chloride (*Mes-NHC, M = Ca, Sr, Ba) [40] or 1,3-bis(2,6-di-isopropylphenyl)imidazolium chloride (Dipp-NHC, M = Mg, Ca, Sr, Ba) [40,43] in toluene or benzene allowed for the isolation of three-coordinate species, $M[N(SiMe_3)_2]_2(NHC)$. The Ca and Sr species display close contacts to one or more methyl groups from the $[N(SiMe_3)_2]^-$ ligand in the form of agostic interactions (Table 5).

Another potential factor in the lack of heavy alkaline earth bis(bis(trimethylsilyl)amide) donor adducts is their strong propensity to cleave ethers, as shown with the treatment of $M[N(SiMe_3)_2]_2(thf)_2$ solutions with the cyclic ethers, 12-crown-4, 15-crown-5, and 18-crown-6 in a 1:1 molar ratio [25]. The reactions were followed by ^1H NMR spectroscopy. In each case the silylamine, $HN(SiMe_3)_2$, was detected along with the formation of vinyl ethers. Similarly, attempts at metallating triphenylmethane with $Sr/Ba[N(SiMe_3)_2]_2$ in the presence of 18-crown-6 produces the dimeric ether scission products $[M(C_{12}H_{23}O_6)(N(SiMe_3)_2)]_2$ [44].

Applications of the alkaline earth silyl amides are far-reaching. Alkaline earth metal silyl amides are one of the most commonly used classes of polar organometallic reagents in organic synthesis including catalytic transformations, enolization reactions, hydroamination reactions and carbon dioxide fixation [2,26,29,45–51]. The alkaline earth metal silyl amides serve as versatile reagents in organic synthesis, while the heavier congeners have provided a long sought access to a range of heavy alkaline earth metal derivatives [2,12]. Other applications include their use as initiators in polymerization reactions for both synthetic and biodegradable polymers [8,27,28,52–61]. The alkaline earth metal silyl amides have also been studied as potential precursors in MOCVD (metal-organic chemical vapor deposition) processes, as their low coordination numbers and relatively low molecular weight were believed to provide good volatility [42,62–64]. However, frequent silicon incorporation into the resulting films rendered the precursor materials non-ideal [62–64].

In order to further study the effects of ligand bulk on the chemistry of alkaline earth metal amides, the modification of the $[N(SiMe_3)_2]^-$ ligand has become a growing area of interest. These modifications vary from altering the substitution on the $-SiMe_3$ moieties to completely replacing the silyl groups by alkyl and aryl functionalities.

Replacement of one of the methyl groups by *tert*-butyl to afford the $HN(SiMe_3)(SiMe_2{}^tBu)$ ligand, has resulted in a series of Mg and Ca amides [65,66]. Salt metathesis (Scheme 2, Route i) led to the three-coordinate, $Mg[N(SiMe_3)(SiMe_2{}^tBu)]_2(pyr)$ showing that a slight increase in the steric bulk of the ligand has a profound effect on overall metal coordination. In agreement with the lower coordination number on the metal center, the M–N bond distances are shorter (1.991(9) Å), as compared to the four-coordinate $Mg[N(SiMe_3)_2]_2(pyr)_2$ (2.029(1) Å) [41].

For the larger metal center calcium, four-coordinate species were obtained $Ca[N(SiMe_3)(SiMe_2{}^tBu)]_2(donor)_2$ (donor = pyridine, hexamethylphosphoric acid triamide (HMPA) and 4-dimethylaminopyridine (DMAP)) [66]. Despite the slight increase in steric bulk of the ligand, the compounds display quite similar structural features compared to the THF adduct $Ca[N(SiMe_3)_2]_2(thf)_2$ [38]. In addition, all three of these calcium compounds display agostic interactions (M···H–C) from the methyl groups (Table 6) stabilizing the metal center.

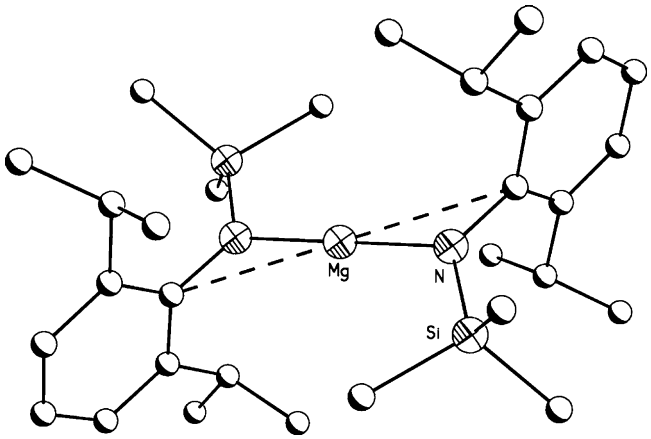

Fig. 3. Structure of $Mg[N(SiMe_3)(Dipp)]_2$ [67]. Hydrogen atoms removed for clarity. M···C(π) interactions shown as dashed lines.

Further increase in ligand bulk in $HN(SiMe_3)(SiPh_2{}^tBu)$, afforded a rare monomeric three-coordinate species for calcium, $Ca[N(SiMe_3)(SiPh_2{}^tBu)]_2(thf)$ (Scheme 2, Route i) [66]. The only other monomeric examples of three-coordinate heavy alkaline earth metal amides are the aforementioned NHC adducts $M[N(SiMe_3)_2]_2(NHC)$ [40]. In this case, the sterically encumbering ligand and not the size of the donor allows for metal stabilization. This is further evidenced by the crowded ligand affording several secondary interactions to help stabilize the metal center including M···C(π) contacts from the phenyl substituents and both M···H–C and M···C interactions (Table 6).

In line with decreasing metal size, for magnesium, a rare, two-coordinate species is obtained, $Mg[N(SiMe_3)(SiPh_2{}^tBu)]_2$, where the metal center is stabilized through M···C(π) contacts (Table 6) from the phenyl substituents and a N–M–N angle of 140.15(6)° (Scheme 2, Route vi) [65]. The deviation from a linear N–M–N geometry is attributed to M···C(π) interactions. A similar deviation is also seen for magnesium using the $[N(SiMePh_2)_2]^-$ ligand, with the donor-free $Mg[N(SiMePh_2)_2]_2$ (Scheme 2, Route vi) [10]. In this rare two-coordinate species, the phenyl groups arrange themselves to result in a N–M–N angle of 162.8(3)°. Again, M···C(π) contacts from the phenyl substituents arise to help stabilize the metal center (Table 6). Along with $Mg[N(SiMe_3)(Dipp)]_2$ [67], (Dipp = 2,6-di-isopropyltrimethylsilylphenyl) which will be described in a subsequent section, $Mg[N(SiMe_3)(SiPh_2{}^tBu)]_2$ and $Mg[N(SiMePh_2)_2]_2$ represent the only three examples of two-coordinate magnesium amides. Replacement of all methyl substituents from a $-SiMe_3$ moiety by phenyl substituents affords a four-coordinate species $Ca[N(SiMe_3)(SiPh_3)]_2(thf)_2$ (Scheme 2, Route i), where M···C(π) and M···H–C agostic interactions arise further stabilizing the metal center (Table 6) [66].

Silylated amine ligands where one of the silyl groups has been replaced by an aryl substituent such as 2,4,6-trimethylaniline (Mes) or 2,6-di-isopropylaniline (Dipp) provided detailed insight into the effect of ligand size on compound geometry. In the case of $HN(SiMe_3)(Dipp)$, the steric demand of the ligands is substantial, allowing the isolation of the donor-free, two-coordinate $Mg[N(SiMe_3)(Dipp)]_2$ (Fig. 3) (Scheme 2, Route vi) displaying a linear N–M–N angle [67]. Close contacts in the form of M···C(π) interactions, arise to saturate the metal center as also observed for the previous two-coordinate magnesium species [10,65]. How-

Table 5
Reported secondary interactions for $M[N(SiMe_3)_2]_2(NHC)_2$.

	CN	M···C (Å)	References
$Ca[N(SiMe_3)_2]_2(Mes\text{-}NHC)_2$	3+1	2.598(2)	
$Sr[N(SiMe_3)_2]_2(Mes\text{-}NHC)_2$	3+1	2.731(3)	[40]
$Ca[N(SiMe_3)_2]_2(Dipp\text{-}NHC)_2$	3+2	2.893(2)–2.913(2)	

*Mes-NHC = 1,3-bis(2,4,6-trimethylphenyl)imidazolium; Dipp-NHC = 1,3-bis(2,6-di-isopropylphenyl) imidazolium.

Table 6
Reported secondary interactions for substituted silylamides.

	CN	M···H–C (Å)	M···C (Å)	M···C(π) (Å)	References
$Mg[N(SiMePh_2)_2]_2$	2+4			2.65–2.96	[10]
$Mg[N(SiMe_3)(SiPh_2{}^tBu)]_2$	2+3			2.558(2)–2.646(2)	[65]
$Ca[N(SiMe_3)(SiMe_2{}^tBu)]_2(pyr)_2$	4+3	2.89(4)–2.70(3)			
$Ca[N(SiMe_3)(SiMe_2{}^tBu)]_2(hmpa)_2$	4+4	2.72(5)–2.86(5)			
$Ca[N(SiMe_3)(SiMe_2{}^tBu)]_2(dmap)_2$	4+3	2.71(3)–2.92(4)			[66]
$Ca[N(SiMe_3)(SiPh_2{}^tBu)]_2(thf)$	3+5	2.643(19)	3.236(2)	3.184(2)–2.855(2)	
$Ca[N(SiMe_3)(SiPh_3)]_2(thf)_2$	4+2		3.141(3)–3.142(3)		

Table 7
Reported secondary interactions for substituted silylamides.

	CN	M···H–C (Å)	M···C (Å)	M···C(π) (Å)	References
$Mg[N(SiMe_3)(Dipp)]_2$	2+2		2.861(1)		[67]
$Mg[N(SiMe_3)(Dipp)]_2(Et_2O)$	3+1		2.799(2)		[68]
$Ca[N(SiMe_3)(Mes)]_2(tmeda)$	4+2	2.77			[18]
$Sr[N(SiMe_3)(Mes)]_2(thf)_2$	4+4	2.788		2.884(2)–3.105(2)	[19]
$Sr[N(SiMe_3)(Mes)]_2(pmdta)$	5+4	2.904–3.213			[18]
$Ba[N(SiMe_3)(Mes)]_2(thf)_3$	5+5	3.120–3.212		3.140(2)–3.205(2)	[19]
$Ba[N(SiMe_3)(Mes)]_2(tmeda)$	4+2	2.78			[18]
$Ba[N(SiMe_3)(Mes)]_2(pmdta)$	5+5	2.84–3.23			
$Sr[N(SiMe_3)(Dipp)]_2(thf)_2$	4+2	2.933–3.178			[67]
$Ba[N(SiMe_3)(Dipp)]_2(thf)_2$	4+2	2.987–3.188			
$Sr[N(SiMe_3)(Dipp)]_2(hmpa)_2$	4+4	2.832–2.943			[69]
$Ba[N(SiMe_3)(Dipp)]_2(hmpa)_2$	4+3	2.899–3.137			

ever, in the presence of diethylether, the thee-coordinate adduct, $Mg[N(SiMe_3)(Dipp)]_2(Et_2O)$ (Fig. 4) [68] is obtained along with a single M···C(π) interaction (Table 7), while in THF the heteroleptic species, $[(^nBu)Mg\{N(SiMe_3)(Dipp)\}thf_2]$, is isolated [67]. Use of this ligand for the heavier metals afforded bis-THF solvated four-coordinate compounds of the form $M[N(SiMe_3)(Dipp)]_2(thf)_2$ (M = Ca, Sr, Ba) (Scheme 2, Route vi) [67]. Both the strontium and barium compounds display agostic interactions (M···H–C) arising from the isopropyl substituents, in order to fully saturate the metal centers (Table 7).

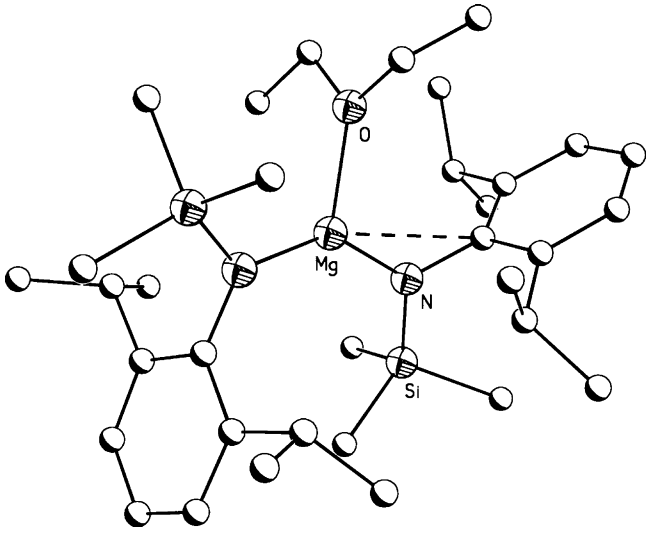

Fig. 4. Structure of $Mg[N(SiMe_3)(Dipp)]_2(Et_2O)$ [68]. Hydrogen atoms removed for clarity. M···C(π) interactions shown as dashed lines.

More recently, our group has isolated a family of magnesium amides based on the $[N(SiMe_3)(R)]^-$ ligand system, with R = $SiMe_3$, C_6H_5 (aniline), 2,4,6-trimethylphenyl (Mes) and 2,6-di-isopropylphenyl (Dipp) in conjunction with HMPA, allowing the investigation of ion-association in the context of steric saturation. Contact four-coordinate species are observed for $Mg[N(SiMe_3)_2]_2(hmpa)_2$, $Mg[N(SiMe_3)(Ph)]_2(hmpa)_2$, and $Mg[N(SiMe_3)(Mes)]_2(hmpa)_2$ (Scheme 2, Route vi) [70]. On average, shorter M–O bond lengths were observed for the HMPA adducts as compared to the respective THF adducts. This is attributed to HMPA being a stronger Lewis base than THF.

In the case of $[N(SiMe_3)(Dipp)]^-$, the unusual partially separated $[Mg\{N(SiMe_3)(Dipp)\}(hmpa)_3][N(SiMe_3)(Dipp)]$ is providing the first example of an alkaline earth separated amido species (Fig. 5) [70]. Highlighting the unique coordination mode of this compound, examples of separated amides in early main group chemistry are limited to alkali metal species, including $[Li(12\text{-crown-}4)_2][N(SiPh_3)_2]\cdot THF$ [9,71], $[K(18\text{-crown-}6)N(Ph)_2]$ [72], and $\{[K(18\text{-crown-}6)N(SiMePh_2)_2]\}_\infty$ [73]. For the heavier metals Sr and Ba, the combination of the $^-[N(SiMe_3)(Dipp)]$ with HMPA allowed the isolation of the four-coordinate contact molecules $M[N(SiMe_3)(Dipp)]_2(hmpa)_2$ (M = Sr, Ba) [69]. The species display agostic interactions from the ligand isopropyl groups (Table 7).

Analogous studies with the smaller $HN(SiMe_3)(Mes)$ ligand, also afforded compounds of the form $M[N(SiMe_3)(Mes)]_2(donor)_n$ (THF, n = 2, Mg, Ca, Sr; n = 3 Ba; TMEDA, n = 1, Ca, Ba; PMDTA, pentamethyldiethylenetriamine, n = 1, Sr, Ba) (Scheme 2, Route vi,

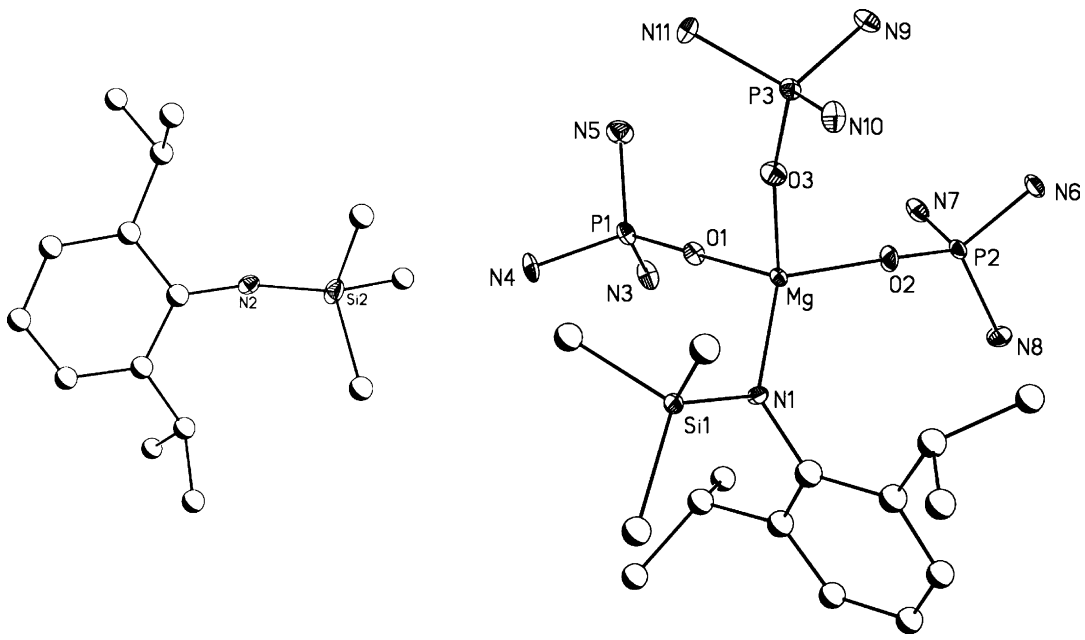

Fig. 5. Structure of [Mg{N(SiMe$_3$)(Dipp)}(hmpa)$_3$][N(SiMe$_3$)(Dipp)] [70]. Methyl groups from HMPA and hydrogen atoms removed for clarity.

M = Mg, Route i, M = Ca–Ba) [19,18], where a significant number of agostic interactions arising from both ligands and donors serve to stabilize the metal centers (Table 7). The differences in ligand bulk between the Dipp and Mes ligands are impressively reflected by the significant change in reactivity, with compounds bearing the smaller mesityl ligand being much more reactive.

Replacement of one of the –SiMe$_3$ moieties by either an isopropyl (^{i}pr), cyclohexyl (cy), benzyl (bz), 2,6-di-isopropylphenyl (Dipp), or adamantyl (ad) in the presence of donors leads to a series of magnesium compounds, however this chemistry has not been extended to the heavier metals. Examples include species for magnesium of the type Mg[N(SiMe$_3$)(R)]$_2$(donor)$_2$, (R = ^{i}Pr, donor = 4-dimethylaminopyridine (DMAP), R = Cy, donor = DMAP; R = Bz, donor = HMPA, DMAP, R = ad-Dipp, donor = THF) [65,74]. Not surprisingly, aggregation occurs in the absence of donors, as seen for [Mg{N(SiMe$_3$)(Cy)}$_2$]$_2$. If an adamantyl group replaces a –SiMe$_3$ moiety in conjunction with magnesium, a three-coordinate species is isolated in Et$_2$O, Mg[N(SiMe$_3$)(ad)]$_2$(Et$_2$O) [65]. A four coordinate species is also obtained in Mg[N(Si^{t}BuMe$_2$)(2-pyridylmethyl)]$_2$ where the pyridyl substituent acts as an intramolecular donor [75]. Finally, further reducing the steric demand of the –SiMe$_3$ moiety in the ligand [HN(SiMe$_2$H)(^{t}Bu)]$_2$ results in dimer formation for magnesium, {Mg[N(SiMe$_2$H)(^{t}Bu)]$_2$}$_2$ [76]. The compound exhibits an agostic interaction (Mg···C, 2.98 Å) from one of the methyl groups of the –^{t}Bu substituent from the bridging ligand, while also displaying Mg···H–Si agostic interactions, 2.49 and 2.22 Å from both bridging and terminal hydrogens from the –SiMe$_2$H substituents.

2.2. Secondary non-silylated amines

Very recently, amido chemistry involving the alkaline earth metals has seen the first non-silylated monomeric heavy alkaline earth amido species. Westerhausen et al. were able to synthesize alkaline earth diphenylamides, M(N(Ph)$_2$)$_2$(donor)$_x$, (donor = THF, HMPA, Mg, x = 2; Sr, Ba, x = 4; donor = DME, Ca, x = 2) (Scheme 2, Route vi = Mg, Route i, vii, ix = Ca, Route i = Sr–Ba) which surprisingly exhibit good solubility likely due to the monomeric nature of the complexes [77,78]. The increase in overall coordination numbers as compared to the HMDS derivatives is attributed to lack of steric bulk afforded by the diphenylamide ligand. Further stabilization is provided by a number of M···C(π) interactions (Table 8). The sterically encumbering HMPA provided the stabilization necessary to isolate Mg(N(Ph)$_2$)$_2$(hmpa)$_2$ via a disproportionation reaction [78]. Similarly, replacement of a phenyl group from the diphenylamide ligand with ^{i}Pr resulted in the monomeric five-coordinate Ca[N(^{i}Pr)(Ph)]$_2$(thf)$_3$ [79], while replacement with a smaller methyl group, resulted in a monomeric six-coordinate species, Ca[N(Me)(Ph)]$_2$(thf)$_4$ [80].

While replacement of –SiMe$_3$ by less sterically demanding phenyl groups still afforded monomeric complexes, the corresponding magnesium dibenzylamides were solvent and donor-dependent. In the absence of polar solvents, a three-coordinate magnesium dimer, [Mg{N(CH$_2$Ph)$_2$}$_2$]$_2$ is isolated [81]. Addition of 2 molar equivalents of either THF or HMPA led to the coordination of one donor molecule per magnesium resulting in the dimeric [Mg{N(CH$_2$Ph)$_2$}$_2$(donor)]$_2$ (donor = THF, HMPA) [81]. Addition of excess HMPA or THF affords the monomeric Mg[N(CH$_2$Ph)$_2$]$_2$(donor)$_2$ as evidenced by NMR spectroscopy. Demonstrating the propensity for four-coordinate species, addition of two molar equivalents of TMEDA yielded the monomeric Mg[N(CH$_2$Ph)$_2$]$_2$(tmeda) [81]. Similar results were obtained in the presence of dicyclohexylamine, HN(Cy)$_2$, affording the three-coordinate magnesium dimer, [Mg(N(Cy)$_2$)$_2$]$_2$, a rare example of a homoleptic dialkylmagnesium amide [82]. For the smaller metal beryllium, use of the small dimethylamine amine ligand led to the trimeric species, {Be[N(CH$_3$)$_2$]$_2$}$_3$ [83–85].

2.3. Primary amines

Despite plentiful examples of monomeric alkaline earth secondary amide compounds [7,18,67], much less is known about the corresponding primary amides. Among these, the few examples

Table 8
Reported secondary interactions for M[N(Ph)$_2$]$_2$(donor)$_x$.

	CN	M···C(π) (Å)	References
Ca[N(Ph)$_2$]$_2$(dme)$_2$	6 + 1	3.174(2)	
Sr[N(Ph)$_2$]$_2$(thf)$_4$	6 + 1	3.236(2)	[77]
Ba[N(Ph)$_2$]$_2$(thf)$_4$	6 + 1	3.293(4)	

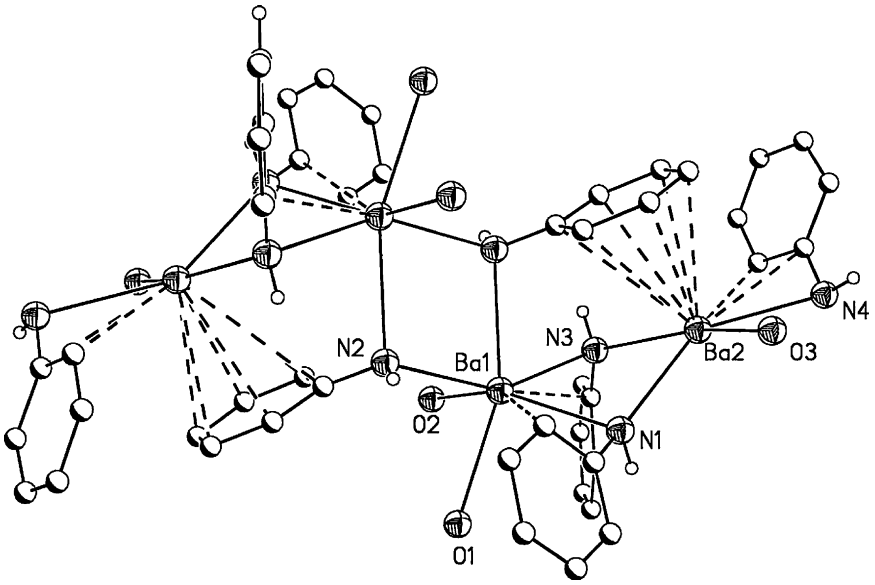

Fig. 6. Structure of $[(THF)_{1.5}Ba\{N(H)Ph\}_2]_\infty$ [91]. Hydrogen atoms except acidic protons removed for clarity. M···C(π) interactions shown as dashed lines.

reported have all been oligomeric or display extended structures [80,86–91]. The original heavy alkaline earth primary amides, the $M(NH_2)_2$ (M = Ca, Sr, Ba) are easily obtained from dissolving the metals in liquid ammonia [86–90]. The calcium and strontium species crystallized with six-coordinate metal centers, while the larger barium species display coordination numbers of up to eight. The low solubility of the compounds made further characterization and the subsequent use of the compounds in synthetic applications very difficult.

Only four examples of the lighter metal magnesium have been reported as monomeric homoleptic primary amido species bearing either a very bulky substituted phenylamide, as seen in $Mg[N(H)(Triph)]_2(thf)_2{\cdot}THF$ (Triph = 2,4,6-triphenylaniline) or employing the Lewis base HMPA, in $Mg[N(H)(Mes)]_2(hmpa)_2$ [82] and $Mg[N(H)(Mes^*)]_2(hmpa)_2$, (Mes* = 2,4,6-tri-*tert*-butylaniline) (Scheme 2, Route vi) [92]. A similar approach was used by Westerhausen et al. with the use of bidentate TMEDA to isolate $Mg[N(H)(Si^iPr_3)]_2$(tmeda) [93]. The aforementioned compounds are all monomeric in nature, however when pentafluroaniline, $H_2N(Ar_F)$ is employed in the presence of THF, a trimer is obtained where each Mg atom is bridged by three μ_2-anions, $[\{(Ar_FNH)_6Mg_3{\cdot}(thf)_6\}{\cdot}2Tol{\cdot}THF]$ [94].

The Westerhausen group reported on a series of primary anilides, $[(THF)_xM\{N(H)Ph\}_2]_y$ ($x = 2$, $y = 4$ (Ca); = 2, ∞ (Sr); = 1.5, ∞ (Ba) Fig. 6) (Scheme 2, Route vii = Mg, Ca, Route i Ca, Sr, Ba, Route ii = Sr, Ba) where the small size of the ligands rendered polymeric species and the reduced amount of co-ligand in the barium species is explained by additional Ba···C(π) contacts [91]. An increase in ligand size to $[N(H)Mes]^-$ led to a reduction in aggregation with the trimeric $(THF)_6Ca_3[N(H)Mes]_6$ (Mes = 2,4,6-trimethylaniline). Introduction of fluoro functionalities in the ligand further suppressed aggregation through a host of non-covalent M···F interactions as seen in the dinuclear $(THF)_5Ca_2[N(H)\text{-}2,6\text{-}F_2C_6H_3]_4{\cdot}2THF$, the dinuclear $(THF)_6Sr_2[N(H)\text{-}2,6\text{-}F_2C_6H_3]_3I{\cdot}THF$, and the polymeric $[(THF)_2Ba\{N(H)\text{-}2,6\text{-}F_2C_6H_3\}_2]_\infty$ (Scheme 2, Route I, Ca, Sr, Ba). Due to their highly aggregated nature, the compounds display poor solubility in organic solvents [80].

More recently, through the use of the sterically demanding HMPA co-ligand, our group has been able to isolate a unique family of monomeric heavy alkaline earth primary amides, $M[N(H)(Dipp)]_2(hmpa)_3$ (M = Ca, Sr, Ba, Fig. 7) (Scheme 2, Route i) [95]. As the compounds are highly reactive, synthesis and work-up need to be done in 24 h. These isostructural compounds display distorted trigonal bipyramidal geometries with a formal coordination number of 5. An increasing number of secondary non-covalent agostic interactions (M···H–C) arise from the alkyl groups from the aryl substituents to fully saturate the coordination spheres of the metals (Table 9). Further metal stabilization is achieved through agostic interactions from the N–H moiety from the primary amide.

The presence of these agostic interactions was detected both crystallographically and spectroscopically through the use of variable low-temperature VT ^1H NMR experiments [96–101]. Upon cooling, peak splitting was observed due to hindered rotations from the presence of agostic interactions. Energies of rotation were calculated to be 13.72 and 20.16 kcal mol^{-1} for calcium and barium respectively [95]. These values are in accordance with those found for a previously reported secondary amide $Sr[N(SiMe_3)(Mes)]_2$(pmdta), where values of 14.60 and 13.64 kcal mol^{-1} were observed due to agostic interactions from the *o*-methyl substituent and from a trimethylsilyl group [18].

Employment of the multidentate chelating donor 18-crown-6 in conjunction with the $H_2N(Dipp)$ ligand affords, $Ba[N(H)(Dipp)]_2$(18-crown-6) (Fig. 8), where the 18-crown-6 envelops the metal center in the equatorial plane, while the ligands are *trans* to each other with a N–M–N angle of 157.08(15)° [95]. The overall increase in coordination number by using the multidentate donor results in a lower number of agostic interactions (8 + 2) as compared to $Ba[N(H)(Dipp)]_2(hmpa)_3$ (5 + 6) (Table 9).

In the case of the less sterically encumbering ligand $H_2N(Mes)$, only the Ca derivative $Ca[N(H)(Mes)]_2(hmpa)_3$, was obtained [95]. The compound also displays a large number of agostic interactions originating from the methyl substituents from the aryl group (Table 9). Collectively, the primary amido compounds demonstrate that the lack of steric bulk on the ligand has a profound effect on metal stabilization, resulting in oligomerization and/or the emergence of secondary interactions in order to achieve steric saturation.

2.4. Imides

Alkaline earth metal imides are rare and limited to magnesium compounds and are oligomeric in nature. Equimolar alkane elimination conditions (Scheme 2, Route vi) between primary

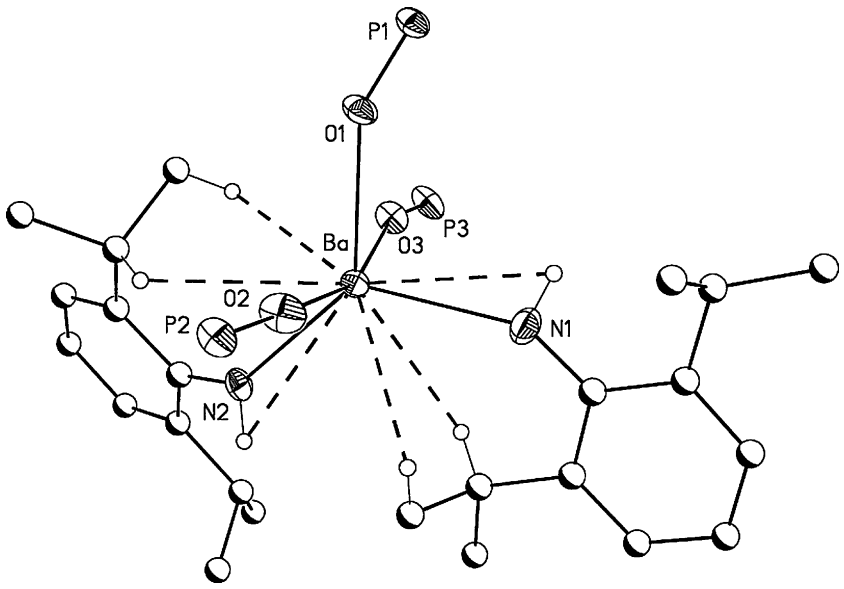

Fig. 7. Structure of Ba[N(H)(Dipp)]$_2$(hmpa)$_3$ [95]. Hydrogen atoms not involved in agostic interactions and methyl groups from HMPA removed for clarity. Agostic interactions shown as dashed lines.

Table 9
Reported secondary interactions for M[N(H)(R)]$_2$(donor)$_3$.

	CN	M···H–C (Å)	M···H–N (Å)	References
Ca[N(H)(Mes)]$_2$(hmpa)$_3$	5 + 4	2.952–3.004	2.735–2.767	
Ca[N(H)(Dipp)]$_2$(hmpa)$_3$	5 + 4	2.753–2.764	2.752–2.785	
Sr[N(H)(Dipp)]$_2$(hmpa)$_3$	5 + 5	2.846–3.018	2.902–2.921	[95]
Ba[N(H)(Dipp)]$_2$(hmpa)$_3$	5 + 6	2.904–3.213	3.004–3.147	
Ba[N(H)(Dipp)]$_2$(18-crown-6)	8 + 2		2.967–3.045	

R = Mes = 2,4,6-trimethylaniline; Dipp = 2,6-di-isopropylaniline.

amines and Bu_2Mg were used to synthesize [(thf)Mg(N(Ph))]$_6$, [(thf)MgN(1-naphthyl)]$_6$, and [(hmpa)MgN(1-naphthyl)]$_6$ [102,103]. All three complexes adopt a prismatic hexameric arrangement in the solid state and have been studied as possible imide transfer reagents towards the synthesis of main group imido compounds [102].

Hexameric imides are also obtained with the use of 2,3,4,5,6-pentafluroaniline, $H_2N(Ar_F)$ in THF and dioxane resulting in [(donor)MgNAr$_F$]$_6$ [94]. Tetrameric magnesium imides are isolated with $H_2NSi(Ph)_3$ and 2,4,6-trichloroaniline, $H_2N(Ar_{Cl})$ in the presence of either THF or dioxane, yielding [(thf)MgNSi(Ph)$_3$]$_4$, [(thf)MgN(Ar$_{Cl}$)]$_4$, and [(diox)MgN(Ar$_{Cl}$)]$_4$ [94,104]. These have been studied as desirable candidates as preassembled secondary building units to construct metal-organic frameworks or coordination polymers [94].

2.5. Heteroleptic amides

A range of heteroleptic organomagnesium amides have been isolated where incomplete elimination of both organogroups

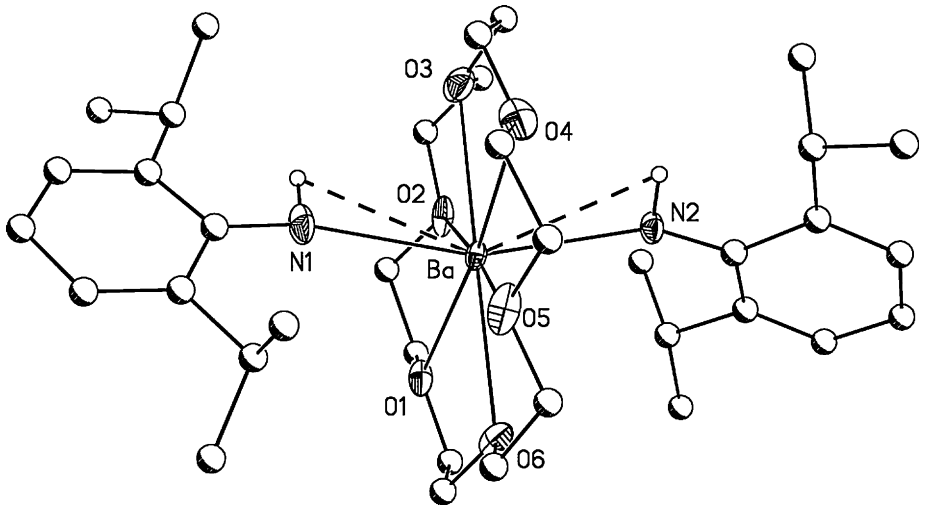

Fig. 8. Structure of Ba[N(H)(Dipp)]$_2$(18-crown-6) [95]. Hydrogen atoms except acidic protons removed for clarity. Agostic interactions shown as dashed lines.

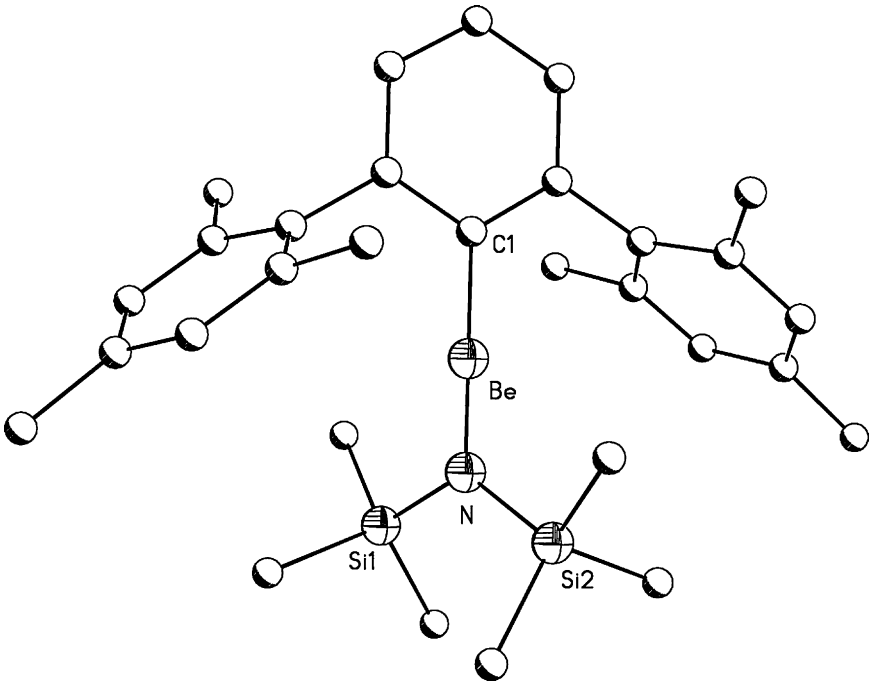

Fig. 9. Structure of Be[C_6H_3-2,6-Mes_2][$N(SiMe_3)_2$] [108]. Hydrogen atoms removed for clarity.

is observed as in the dimeric [{(^{s}Bu)Mg(μ-$N(SiMe_3)_2$)}$_2$] [27]. Heteroleptic products are commonly obtained by metallation of organomagnesium alkanes with amines (Scheme 2, Route vi). When sterically demanding silylamines are employed, the reactions are solvent dependent, with ethereal solvents affording heteroleptic products including monomeric [(^{n}Bu)Mg{$N(SiMe_3)$(Dipp)}thf_2] [67], [(R)M{$N(Ph)_2$}$(thf)_2$] (R = Et, ^{i}Pr) [78] and [(^{n}Bu)Mg{N(H)(Dipp)}tmeda] [105]. Dimeric species have also been isolated with [{(μ-Me)Mg{N(H)(Si^iPr_3)}thf_2] [93] and [{(^{n}Bu)Mg(μ-N(H)(^{t}Bu))$_2$$thf_2$] [82] displaying a M_2N_4 core similar to the [M{$N(SiMe_3)_2$}$_2$] dimers.

Reactions of [(Cp)MgMe(Et_2O)]$_2$ with the corresponding amines resulted in a series of dimeric compounds of the form [{(η^5-Cp)Mg(μ-NR_2)$_2$}$_2$] (R = $N(Ph)_2$, N(H)(Dipp), N(H)($CH(CH(CH_3)_2)_2$), $N(CH(CH_3)_2)(CH_2Ph)$) [106]. In each case, the Cp is in the terminal position, while the amido ligand is bridging between metal centers. Dimer formation is also seen for a series of Cp (cyclopentadienyl) containing compounds. Reactions of ^{t}BuLi with ^{n}BuMgNR_2 (R = $N(SiMe_3)_2$, $N(^iPr)_2$, $N(CH_2Ph)_2$, 2,2,6,6-tetramethylpiperidide (TMP)) led to the isolation of a series of dimers with the general formula [{(^{t}Bu)Mg(μ-NR_2)$_2$}$_2$] where the larger amide ligands bridge the metal centers [105]. In the case of the TMP ligand, agostic interactions were observed arising from the methyl groups of the bridging ligand.

Reactions of Mg[$N(SiMe_3)_2$]$_2$ with $H_2N(Ph)$ result in [{Mg(μ-N(H)(Ph))($N(SiMe_3)_2$)thf_2}], where the primary amide is bridging the metal centers [107]. However, when Mg[$N(SiMe_3)_2$]$_2$ is reacted with the slightly larger H_2N(Dipp) primary amine, the donor-free trimer, Mg_3(μ-N(H)(Dipp))$_4$($N(SiMe_3)_2$)$_2$, is obtained despite the presence of THF in the reaction [82]. Finally, a dodecamer, {Mg[Et][N(H)(Dipp)]}$_{12}$, is obtained if H_2N(Dipp) is reacted with Et_2Mg [82].

In the case of beryllium, both dimeric and monomeric species can be isolated through the use of a sterically encumbering terphenyl ligand, C_6H_3-2,6-Mes_2 in combination with a series of primary and secondary amines [108]. Use of the aniline ligand leads to a dimeric species, {Be[C_6H_3-2,6-Mes_2][μ-N(H)(Ph)]}$_2$ with the terphenyl ligand in the terminal position [108]. Increasing the bulk of the primary amine to $H_2NSi(Ph)_3$, results in a three-coordinate monomer, Be[C_6H_3-2,6-Mes_2][N(H)($Si(Ph)_3$)](Et_2O) [108]. Finally, use of the sterically encumbering [$N(SiMe_3)_2$]$^-$ affords to the first example of a two-coordinate beryllium center in the solid state, Be[C_6H_3-2,6-Mes_2][$N(SiMe_3)_2$] (Fig. 9), displaying a 180° C–Be–N angle [108].

For the heavier calcium, reactions of a heavy Grignard reagent RCaI (R = Ph, napthyl (naph)) with $KN(SiMe_3)_2$ lead to five-coordinate monomeric calcium species, Ca[R][$N(SiMe_3)_2$]$(thf)_3$ [109,110]. Heteroleptic species for calcium and strontium have also been obtained from desilylation reactions involving reactions of the [$N(SiMe_3)$(Dipp/Mes)]$^-$ amine ligands in the presence of HMPA (Scheme 2, Route i). For example, loss of a trimethylsilyl group from one of the ligands results in the heteroleptic primary/secondary amide Ca[$N(SiMe_3)$(Dipp)][N(H)(Dipp)]$(hmpa)_2$ (Fig. 10) [69]. This compound adds to a small group of unsupported heteroleptic primary/secondary amides prepared previously in our group: Sr[$N(SiMe_3)$(Mes)][N(H)(Mes)]$(hmpa)_3$ and Ba[$N(SiMe_3)_2$][N(H)(Mes*)](thf) [111]. The M–N bond length for the primary amide in Sr[$N(SiMe_3)$(Mes)][N(H)(Mes)]$(hmpa)_3$ is shorter than for the larger, secondary amides. However, in Ba[$N(SiMe_3)_2$][N(H)(Mes*)]$(thf)_3$ the M–N bond for the bulky 2,4,6-tri-*tert*-butylaniline primary amide is longer than that for the [$N(SiMe_3)_2$]$^-$ amide, a reflection of the increased steric bulk of the 2,4,6-tri-*tert*-butylaniline ligand.

The impact of metal radius on the occurrence of agostic interactions is demonstrated by this series (Table 10), with Ca[$N(SiMe_3)$(Dipp)][N(H)(Dipp)]$(hmpa)_2$ displaying an overall coordination number of four with four additional agostic interactions stabilizing the metal center (2.675–3.005 Å). The strontium compound bearing the smaller mesityl ligand Sr[$N(SiMe_3)$(Mes)][N(H)(Mes)]$(hmpa)_3$, displays a coordination number of five; the result of an additional HMPA molecule coordinating the metal center. Three additional agostic interactions (2.53–2.94 Å) also provide stabilization to the metal center. Finally, Ba[$N(SiMe_3)_2$][N(H)(Mes*)]$(thf)_3$ displays a coordination number of five, with five additional agostic interactions (2.70–3.18 Å) to result in an overall coordination number of 5 + 5.

Table 10
Reported secondary interactions for select heteroleptic primary/secondary amides.

	CN	M···H–C (Å)	M···H–N (Å)	References
$Ca[N(SiMe_3)(Dipp)][N(H)(Dipp)](hmpa)_2$	4+4	2.768–3.005	2.675	[69]
$Sr[N(SiMe_3)(Mes)][N(H)(Mes)](hmpa)_3$	5+3	2.53–2.94		[111]
$Ba[N(SiMe_3)_2][N(H)(Mes^*)](thf)_3$	5+5	2.70–3.18		

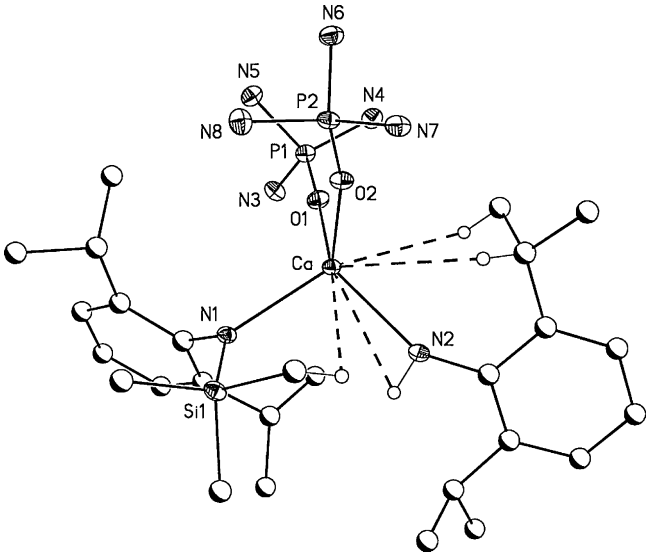

Fig. 10. Structure of $Ca[N(SiMe_3)(Dipp)][N(H)(Dipp)](hmpa)_2$ [69]. Hydrogen atoms not involved in agostic interactions and methyl groups from HMPA removed for clarity. Agostic interactions shown as dashed lines.

A well explored aspect of amido chemistry is the incorporation of the sterically demanding β-diketiminato (BDI) ligand, which has been used to synthesize a number of low coordinate species of main group and transition metals, as reviewed by Lappert among others [8,52,112–118]. As shown in Fig. 11, the ligand can be modified at the backbone and also at the nitrogen atoms in order to modulate electronic and steric properties. Specifically, the BDI ligand with 2,6-di-isopropylphenyl amine has been extensively studied due to ease of synthesis and its ability to achieve steric saturation [8].

More recently, heteroleptic compounds containing BDI and the hexamethyldisilazanide ligand have garnered interest as attractive starting materials in a variety of applications including polymerization initiation [52,114,119]. This is due to the combination of steric demand provided by the BDI ligand with the increased lability of the M–N bond on the $[N(SiMe_3)_2]^-$ ligand. The heavy alkaline earth compounds can be synthesized by a modified salt elimination reaction (Scheme 2, Route i), where two equivalents of $KN(SiMe_3)_2$ are reacted with one equivalent of BDI(H) followed by addition to an alkaline earth metal iodide affording $[(BDI)M\{N(SiMe_3)_2\}(thf)]$ (M = Ca, Sr, Ba) [45]. For the purposes of this review, BDI(H) refers to 2,6-di-isopropylphenyl substituted β-diketimine.

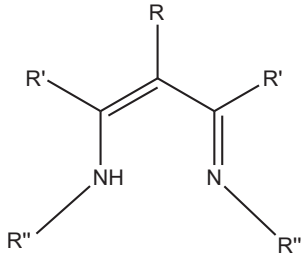

R = H
R' = Me, ^{t}Bu, Ph
R'' = ^{i}Pr, ^{t}Bu ,Ph, Mes, OMes
Dipp, $SiMe_3$

Fig. 11. β-Diketimine (BDI) ligand system.

For the lighter metal magnesium, a 1:1 transamination reaction with BDI(H) in toluene can be employed (Scheme 2, Route viii,) resulting in $[(BDI)Mg\{N(SiMe_3)_2\}]$ [119]. For calcium the THF adduct $[(BDI)Ca\{N(SiMe_3)_2\}(thf)]$ is observed [52,114]. This compound polymerizes *rac*-lactide in THF at room temperature giving static polylactide [52,114]. In correlation with increased metal ionic radii, and increased lability of the M–N $[N(SiMe_3)_2]^-$ bond, the reactivity of these heavier metal compounds increases in comparison to the Mg and Zn analogues [114].

The $[(BDI)Ca\{N(SiMe_3)_2\}(thf)]$ complex has also been used as a stable reaction platform for alkaline earth chemistry with a variety of primary amines and anilines due to its relative solution stability [45]. Addition of stoichiometric amounts of cyclohexylamine ($H_2N(Cy)$) or *t*-butylamine ($H_2N(^tBu)$) resulted in the displacement of THF and formation of the respective amine adducts $[(BDI)Ca\{N(SiMe_3)_2\}(NH_2Cy)]$ characterized by NMR spectroscopy and $[(BDI)Ca\{N(SiMe_3)_2\}(NH_2{}^tBu)]$ characterized by X-ray crystallography. Reactions of $[(BDI)Ca\{N(SiMe_3)_2\}(thf)]$ with methoxymethylamine ($H_2N(CH_2)_2OCH_3$) resulted in the formation of the dimeric primary amide $[(BDI)Ca\{NH(CH_2)_2OCH_3\}]_2$ [45]. Alternatively, treatment of $[(BDI)Ca\{N(SiMe_3)_2\}(thf)]$ with the more sterically demanding $H_2N(Dipp)$ resulted in the elimination of hexamethyldisilazane and the formation of a rare heteroleptic monomeric calcium primary anilide, $[(BDI)Ca\{N(H)(Dipp)\}(thf)]$ [45] (Fig. 12). Aiding in the stabilization of this species is an agostic interaction between the calcium atom and a methine group from one of the isopropyl substituents of the anilide ligand with a value of 2.582 Å. If the less encumbering benzylamine, $H_2N(Bz)$, is used the isostructural dimeric compounds are obtained where the primary amine is bridging the metal centers $[BDIM\{N(H)(Bz)\}]_2$ (M = Mg, Ca) [120,121]. Finally reactions of the heteroleptic species

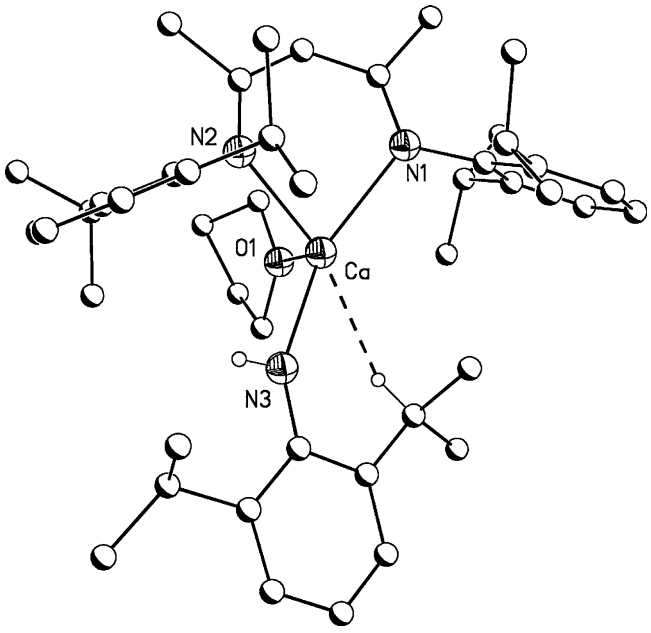

Fig. 12. Structure of $[(BDI)Ca\{N(H)(Dipp)\}(thf)]$ [45]. Hydrogen atoms not involved in agostic interactions removed for clarity. Agostic interactions shown as dashed lines.

[(BDI)Ca{N(SiMe$_3$)$_2$}(thf)] with ammonia gas resulted in the dimer [(BDI)Ca{NH$_2$}(NH$_3$)$_2$]$_2$ [122].

The BDI ligand has also proven useful in isolating heteroleptic species of the alkaline earth metals with secondary non-silylated amines. For magnesium, use of the HN(^{i}Pr)$_2$ ligand leads to [(BDI)Mg{N(^{i}Pr)$_2$}(thf)] [113], or the donor free [(BDI)Mg{N(^{i}Pr)$_2$}] monomers [123]. For calcium, use of HN(Ph)$_2$ results in a monomeric species, [(BDI)Ca{N(Ph)$_2$}(thf)] displaying Ca···C(π) from one of the phenyl groups of the amido ligand [124].

3. Alkaline earth heterobimetallic amides

Recently, heterobimetallic amides based on the [N(SiMe$_3$)$_2$]$^-$ ligand have garnered synthetic interest. Alkali-alkaline earth mixed metal amides have solubility in organic solvents and unique reactivity that is markedly different from that of a mixture of the homometallic counterparts [125–132]. Alkaline earth-alkaline earth mixed metal species are less well known and limited to [MgCa{N(SiMe$_3$)$_2$}$_4$] [127].

3.1. Alkali-alkaline earth heterobimetallic amides

The vast majority of heterobimetallic species contain magnesium, with several examples incorporating lithium. Aside from their significant synthetic utility, these compounds shed light onto the ways that both alkali and alkaline earth metal centers achieve coordinative saturation in both the presence and absence of polar solvents. Combination of the solvent-free dimer, Mg[N(SiMe$_3$)$_2$]$_2$, with Li[N(SiMe$_3$)$_2$] in a 1:2 ratio in toluene affords the heterobimetallic [LiMg{N(SiMe$_3$)$_2$}$_3$] [133]. The lithium atom is formally two-coordinate while the magnesium metal center is three-coordinate. The absence of coordinating donor solvents results in close agostic interactions between the lithium metal center and –SiMe$_3$ groups from the bridging ligands. Close contacts for both alkali and alkaline earth metals in reported heterobimetallic compounds are summarized in Table 11. Reactions involving 1:1 molar ratios of ^{n}BuLi and ^{n}Bu$_2$Mg with 2 equivalents of HN(SiMe$_3$)$_2$ in the presence of pyridine, resulted in the formation of the heteroleptic [(pyr)Li(μ-{N(SiMe$_3$)$_2$}$_2$)Mg(^{s}Bu)] [41]. Despite the steric saturation and secondary interactions afforded to the metal centers by the [N(SiMe$_3$)$_2$]$^-$ ligand, this compound is extremely oxygen sensitive, and "scavenges" oxygen to form an "inverse crown ether", of the form [{(Me$_3$Si)$_2$N}$_4$Li$_2$Mg$_2$(O$_2$)$_x$(O)$_y$] [126]. This group of compounds has been studied at length by the Mulvey group. Several excellent review articles are available on the topic and as such the compounds will not be included here [129,134–140,128].

Donor adducts of the above mentioned [LiMg{N(SiMe$_3$)$_2$}$_3$] family include both THF and pyridine. In each case, the donor coordinates to the monocationic lithium atom, [(donor)LiMg{N(SiMe$_3$)$_2$}$_3$] circumventing the need for close Li based agostic interactions [41]. The combination of Mg[N(SiMe$_3$)$_2$]$_2$ and ^{n}BuLi leads to the formation of heteroleptic [Li(μ-{N(SiMe$_3$)$_2$}$_2$)Mg(^{t}Bu)] stabilized through intermolecular Li based agostic interactions [141]. For sodium, combinations of Na[N(SiMe$_3$)$_2$] with ^{t}BuMgCl in the presence of diethyl ether, allowed formation of [(Et$_2$O)Na(μ-{N(SiMe$_3$)$_2$}$_2$)Mg(^{t}Bu)], exhibiting Na based agostic interactions (Table 11) [141].

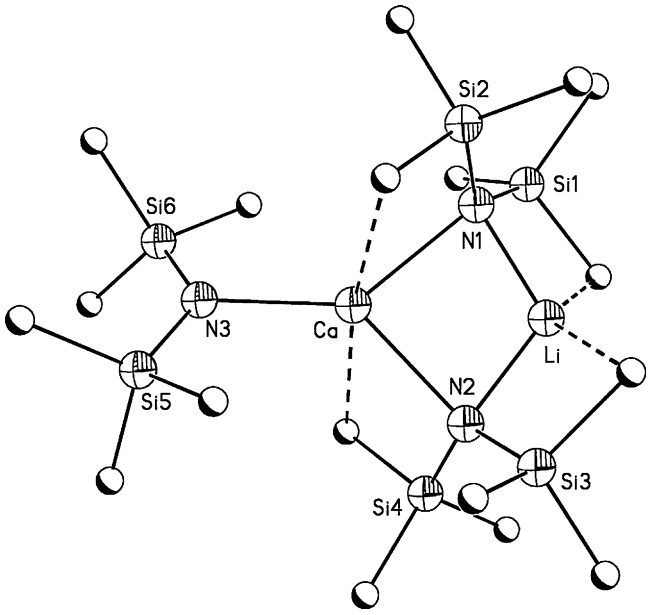

Fig. 13. Structure of [LiCa{N(SiMe$_3$)$_2$}$_3$] [126]. Hydrogen atoms not involved in agostic interactions removed for clarity. Agostic interactions shown as dashed lines.

The combination of Ca[N(SiMe$_3$)$_2$]$_2$ with [Li(N(SiMe$_3$)$_2$)]$_2$ in a 1:1 ratio in toluene, affords the solvent-free [LiCa{N(SiMe$_3$)$_2$}$_3$] (Fig. 13) [126]. This compound is isostructural to the magnesium derivative, however the increase in ionic radii for calcium results in agostic (CN = 6, Mg = 0.72, Ca = 1.00 Å) [3] interactions between the alkaline earth metal center and –SiMe$_3$ groups from the bridging ligands. Li based agostic interactions were also reported (Table 11).

The THF adduct [(thf)LiCa{N(SiMe$_3$)$_2$}$_3$] was obtained by mixing Ca[N(SiMe$_3$)$_2$]$_2$(thf)$_2$ with one equivalent of Li[N(SiMe$_3$)$_2$] in hexane [125]. Shortening of the bridging M–N bonds in this species (2.396(2)) as compared to the homobimetallic [Ca{N(SiMe$_3$)$_2$}$_2$] (2.475(6) Å) [20] suggesting the tilting of the ligands towards the larger alkaline earth metal. This is also supported by widening of the N–M–N angle in the THF adduct (89.9(7)°) as compared to the donor free species (86.57(4)°). However, despite evidence of increased steric crowding around the calcium center, no agostic interactions were reported. The K/Ca derivative [(thf)KCa{N(SiMe$_3$)$_2$}$_3$], was obtained under similar conditions [142]. The larger alkali metal center is saturated by close intermolecular K based agostic interactions from the –SiMe$_3$ groups of the terminal ligand of a neighboring molecule resulting in a polymeric chain structure (Table 11).

Interestingly, attempts to obtain heterobimetallic compounds for the heavier alkaline earth metals only results in

Table 11
Reported secondary interactions for select heterobimetallic amides.

	CN	M(I)···C (Å)	M(II)···C (Å)	References
[LiMg{N(SiMe$_3$)}$_3$]	Li = 2 + 2Mg = 3 + 1	2.294(10)–2.320(9)	2.830(6)	[133]
[Li(μ-{N(SiMe$_3$)$_2$}$_2$)Mg(^{t}Bu)]	Li = 2 + 1 Mg = 3	2.563(3)		[141]
[LiCa{N(SiMe$_3$)}$_3$]	Li = 2 + 2 Ca = 3 + 2	2.368(4)–2.413(4)	2.831(2)–2.859(2)	[126]
[(Et$_2$O)Na(μ-{N(SiMe$_3$)$_2$}$_2$)Mg(^{t}Bu)]	Na = 3 + 2 Mg = 3	2.802 (avg)		[141]
[(thf)KCa{N(SiMe$_3$)}$_3$]	K = 3 + 1 Ca = 3	3.368		[142]
[MgCa{N(SiMe$_3$)$_2$}$_4$]	Mg = 3 Ca = 3 + 2		2.828(5)–2.890(5)	[127]

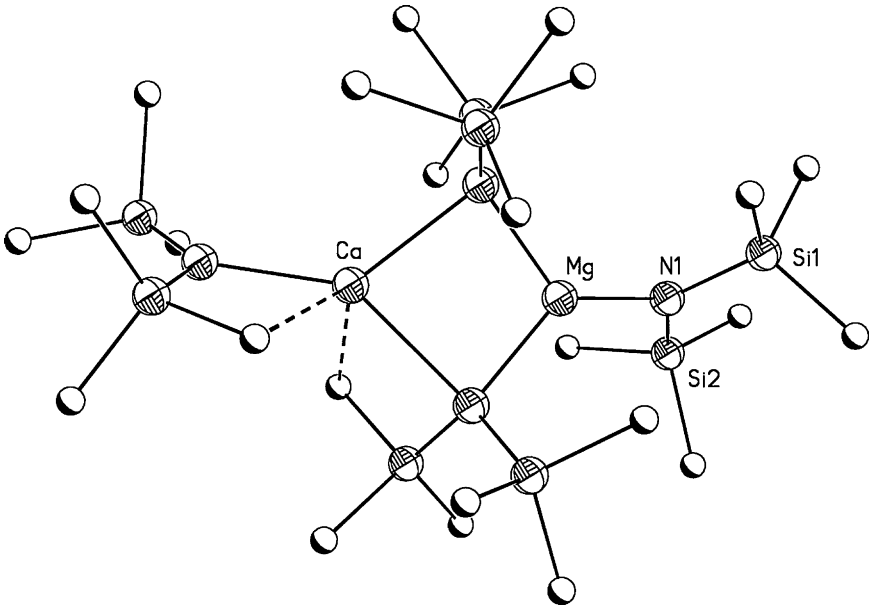

Fig. 14. Structure of $[MgCa\{N(SiMe_3)_2\}_4]$ [127]. Hydrogen atoms not involved in agostic interactions removed for clarity. Agostic interactions shown as dashed lines.

the isolation of the co-crystallization of two neutral products, $[Ba\{N(SiMe_3)_2\}_2(thf)_3][\{Li\{N(SiMe_3)_2\}(thf)\}_2]$ [125]. Possibly, heterobimetallic compounds are not obtained due to the large discrepancy between ionic radii of the metal centers. NMR evidence, based on the treatment of $Na[N(SiMe_3)_2]$ in THF with $Ba[OS(O)_2CF_3]_2$, indicates the formation of the dimeric $[(thf)_2NaBa\{N(SiMe_3)_2\}_3]$, although structural data are not available [143].

Similar structural motifs are observed for alkali-alkaline earth heterobimetallic species containing $HN(CH_2Ph)_2$. In the absence of donors, 1:1 reactions of ^{n}BuLi and ^{n}Bu$_2$Mg resulted in a Mg centered polyhedron, $[Li_2Mg\{N(CH_2Ph)_2\}_4]$, while addition of pyridine led to $[(pyr)LiMg\{N(CH_2Ph)_2\}_3]$ [144]. Use of $HN(Cy)_2$ under similar reaction conditions resulted in $[(thf)LiMg\{N(Cy)_2\}_3]$ after addition of THF [41]. Similar structural motifs are observed for the smaller di-isopropylamine ligand, $HN(^iPr)_2$, where a trio of heterobimetallic species have been isolated: $[\{KMg\{N(^iPr)_2\}_3\}_\infty]$ and $[(tmeda)KMg\{N(^iPr)_2\}_3]$, both stabilized by K agostic interactions and $[(tmeda)NaMg\{N(^iPr)_2\}_3]$ where use of the bidentate donor TMEDA suppresses noncovalent interactions [145].

3.2. Alkaline earth-alkaline earth heterobimetallic amides

The only known example of alkaline earth-alkaline earth heterobimetallic amides is $[MgCa\{N(SiMe_3)_2\}_4]$ (Fig. 14), which hosts a number of intramolecular agostic interactions [127] (Table 11). Addition of pyridine to this species results in asymmetric cleavage of the mixed-metal ring structure, in turn forming a kinetically stable, charge-separated "ate" species of the type $[(Me_3Si)_2NCa(pyr)_n]^+[Mg\{N(SiMe_3)_2\}_3]^-$ observed using ^{1}H NMR spectroscopy. This compound has been studied in enolization reactions [127].

4. Pyrazolates

4.1. Pyrazolate ligand system

Pyrazole is a five-membered ring system containing two adjacent nitrogen atoms. Deprotonation of the pyrazole (pzH) results in a monoanionic aromatic heterocycle, called pyrazolate (pz). Alkyl and aryl substituted pyrazolates have pK_a values in the range of 13–15. The pyrazolate anion can bind to one or more metal centers through one or both of its nitrogen atoms (η^1 and η^2, respectively). In addition, pyrazolates can donate π-electron density to varying degrees (η^3, η^4, and η^5) (Fig. 15). The pyrazolate ligand system is typically substituted with alkyl- and aryl-groups in the 3- and 5-positions to modulate steric bulk, solubility and electronic properties.

Pyrazolate ligands may be substituted in a variety of patterns (Fig. 16). Among the symmetrically substituted pyrazolates, the 3,5-di-*tert*-butylpyrazolate (^{t}Bu$_2$pz) is the most commonly used, as the *tert*-butyl groups increase the steric bulk of the ligand and enhance solubility. Much less prevalent are complexes containing asymmetrically substituted pyrazolates, Group II complexes of unsubstituted pyrazolates have not been reported. Most pyrazolate complexes containing Ca, Sr, and Ba have been pursued in an attempt to find potential CVD precursors with high volatility.

4.2. Symmetrically substituted pyrazolate complexes

4.2.1. 3,5-Dimethylpyrazolate (Me_2pz)

Alkaline earth metal pyrazolates date back to 1995 when the homoleptic "$Ba(Me_2pz)_2$" was obtained by direct metallation, followed by treatment with $GeCl_2$·dioxane. The resulting bimetallic/metalloid complex $Ba[(Me_2pz)_3Ge]_2$·1/2 dioxane, has ligands that are isoelectronic with the scorpionate ligand $[(Me_2pz)_3BH]^-$ [146]. Interestingly, one of the pyrazolyl moieties in each ligand donates π–electron density to the metal and binds in a η^5-fashion, while the other two pyrazolyl moieties are σ-bound through a nitrogen atom (Table 12).

Calcium complexes of the Me_2pz ligand have been reported for a variety of neutral donors, including the monomeric $Ca(Me_2pz)_2$(triglyme), $Ca(Me_2pz)_2$(tetraglyme), and $Ca(Me_2pz)_2$(pmdta) (triglyme = 2, 5, 8, 11-tetraoxadodecane; tetraglyme = 2, 5, 8, 11, 14-pentaoxapentadecane) [147]. Protonated pyrazoles may also act as efficient donors, as shown with the preparation of $[M(Me_2pz)_2(Me_2pzH)_4]$, M = Ca (Fig. 17), Sr [148], stabilized by a hydrogen-bonding embrace between the anionic pyrazolate and the coordinated neutral pyrazole (Table 12). The barium complex, $[\{Ba(Me_2pz)_2(Me_2pzH)_4\}_n]$ could only be isolated as an aggregate with low solubility, limiting characterization. Addition of a number of neutral donors in an attempt to suppress aggregation showed that the polymer could not be broken once

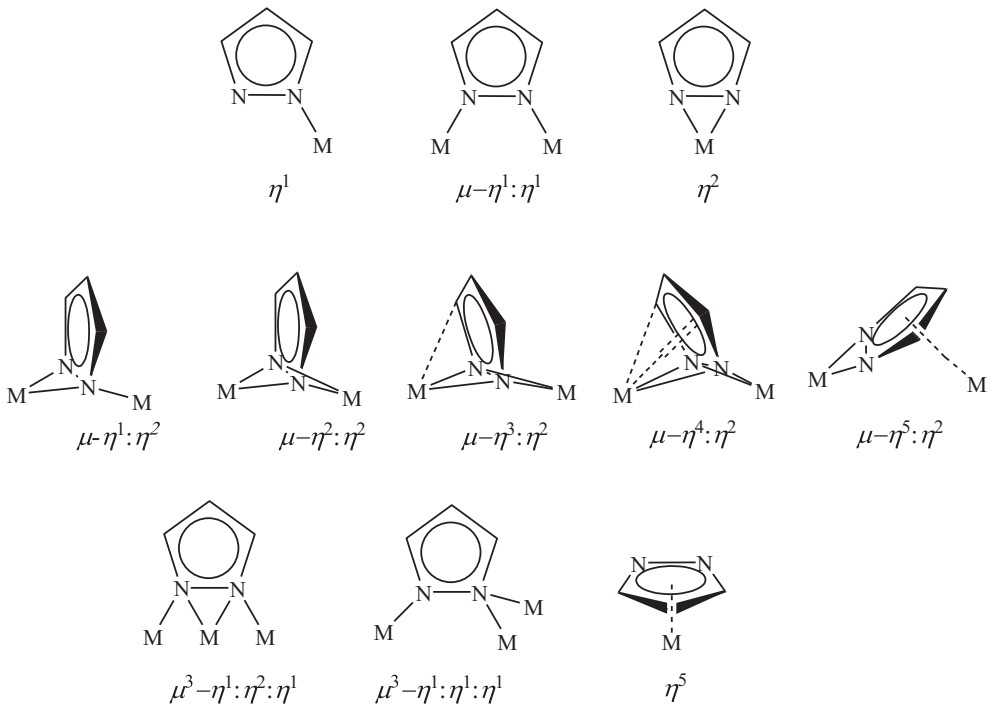

Fig. 15. Pyrazolate binding modes and abbreviations.

formed. Adding PMDTA to the initial reaction mixture resulted in the isolation of the dimeric species [{Ba(Me$_2$pz)$_2$(pmdta)}$_2$] (Fig. 18) [149]. The dimeric barium complex contains two μ-η^2:η^2-bridging pyrazolates that are twisted (but not tilted) to give asymmetric binding to the metal centers. The twisting is caused by steric repulsion between the methyl substituents of the bridging pyrazoles and the PMDTA.

4.2.2. 3,5-Di-isopropylpyrazolate (^{i}Pr$_2$pz)

The ^{i}Pr$_2$pz ligand has an intermediate steric bulk between the Me$_2$pz and Ph$_2$pz. A series of dimeric alkaline earth metal complexes [{Mg(^{i}Pr$_2$pz)$_2$(^{i}Pr$_2$pzH)}$_2$], [{Ca(^{i}Pr$_2$pz)$_2$(^{i}Pr$_2$pzH)$_2$}$_2$], and [{Ba(^{i}Pr$_2$pz)$_2$(py)$_3$}$_2$] were synthesized utilizing Route vi, M = Mg, Route v with ligand Hg(C$_6$F$_5$)$_2$, M = Ca, and Route iii, M = Ba (Scheme 2) [151]. Repeated attempts to form the strontium analogue were not successful. Illustrating steric saturation as the key factor in the coordination chemistry of the target compounds, unreacted ^{i}Pr$_2$pzH was found as the neutral donor in both the Mg and Ca complexes even when excess metal was present during the reaction. A hydrogen embrace was observed for the Mg and Ca complexes similar to that seen above with [Ca(Me$_2$pz)$_2$(Me$_2$pzH)$_4$] and [Sr(Me$_2$pz)$_2$(Me$_2$pzH)$_4$] (Table 12).

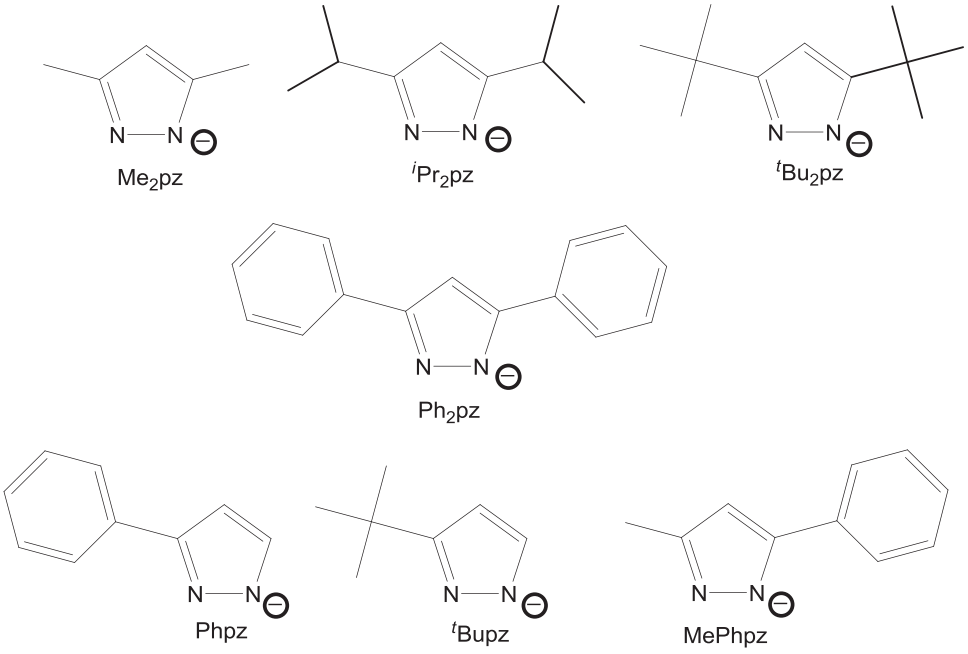

Fig. 16. Pyrazolate substitution patterns and abbreviations.

Table 12
Reported secondary interactions for select compounds.

Compound	CN	M···C(π) (Å)	N···H–N (Å)(°)	References
$[BaTp_2]_2$	8	3.173–3.400		[150]
$Ba[(Me_2pz)_3Ge]_2 \cdot 1/2$ dioxane	12	3.334 (avg)		[146]
$[Ca(Me_2pz)_2(Me_2pzH)_4]$	6		2.01(2), 156(2)°	[148]
$[Sr(Me_2pz)_2(Me_2pzH)_4]$	6		2.02(2), 161(2)°2.06(3), 161(2)°	[148]
$[\{Mg(^iPr_2pz)_2(^iPr_2pzH)\}_2]$	4		1.77, 141°	[151]
$[\{Ca(^iPr_2pz)_2(^iPr_2pzH)_2\}_2]$	7		2.138(3), 147.88°	[151]
$[\{Ba(Ph_2pz)_2(tmeda)\}_2] \cdot TMEDA$	11	3.058(5)–3.281(5)		[149]
$[Mg(^tBu_2pz)_2(^tBu_2pzH)_2]$	4		2.745(17), 153(3)°	[152]
$[Ca_3(^tBu_2pz)_6]$	7	2.804(4)–2.995(4)		[153]
$[Sr_4(^tBu_2pz)_8]$	12, 9	3.029(7)–3.381(9)		[153]
$[Ba_6(^tBu_2pz)_{12}]$	12, 10, 10	3.10(1)–3.39(1)		[153]
$[\{Sr(^tBu_2pz)_2(thf)\}_2]$	8	2.966(2)–3.085(2)		[154]
$[\{Ba(^tBu_2pz)_2(thf)_2\}_2]$	11	3.251(2)–3.499(2)		[154]
$[Ca_2(^tBu_2pz)_3(L^{tBu})]$	9	2.832(2)–2.997(2)		[155]
$[Sr_2(^tBu_2pz)_2(L^{tBu})_2]$	12	3.083(5)–3.229(5)		[155]
$[Ba_2(^tBu_2pz)_2(L^{tBu})_2]$	12	3.189(8)–3.325(8)		[155]

Comparison of $[\{Mg(^iPr_2pz)_2(^iPr_2pzH)\}_2]$, $[\{Ca(^iPr_2pz)_2(^iPr_2pzH)_2\}_2]$ and $[\{Ba(^iPr_2pz)_2(py)_3\}_2]$ illustrates the trend towards increasing hapticity of the bridging pyrazolates as the metal size increases. In $[\{Mg(^iPr_2pz)_2(^iPr_2pzH)\}_2]$ the bridging pyrazolates are only μ-η^1:η^1-bound, but are slightly twisted out of plane to reduce steric interactions between the bridging and terminal ligands. In $[\{Ca(^iPr_2pz)_2(^iPr_2pzH)_2\}_2]$ the bridging pyrazolates are μ-η^1:η^2, avoiding higher hapticity by hydrogen bonding with the bridging pyrazolates (Fig. 19). Finally, the bridging pyrazolates in $[\{Ba(^iPr_2pz)_2(py)_3\}_2]$ are almost perpendicular in the μ-η^2:η^2 mode, yet the need for higher hapticity of the bridging pyrazolates through π-bonding is lessened by the presence of three neutral pyridine donors.

4.2.3. 3,5-Diphenylpyrazolate (Ph_2pz)

The Ph_2pz ligand system has also been used to prepare complexes of the heavier alkaline earth metals, Ca, Sr, and Ba using a variety of neutral donors. The monomeric series $[M(Ph_2pz)_2(thf)_4]$ (M = Ca, Sr, Ba) (Scheme 2, Route iii, M = Ca, Sr, Ba, Route v with

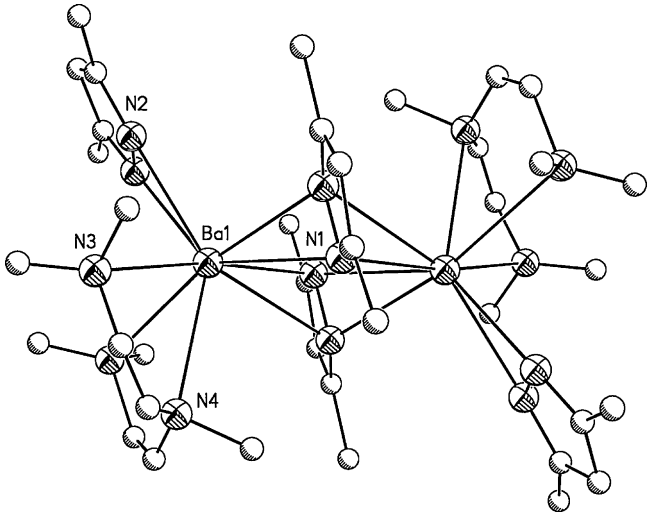

Fig. 18. Structure of $[\{Ba(Me_2pz)_2(pmdta)\}_2]$. Many of the barium pyrazolate complexes display this general dimeric structure, however the binding mode of the bridging pyrazolates often depends on the need for secondary interactions. Here, the bridging pyrazolates are μ-η^2:η^2-bound and twisted [149]. Hydrogen atoms removed for clarity.

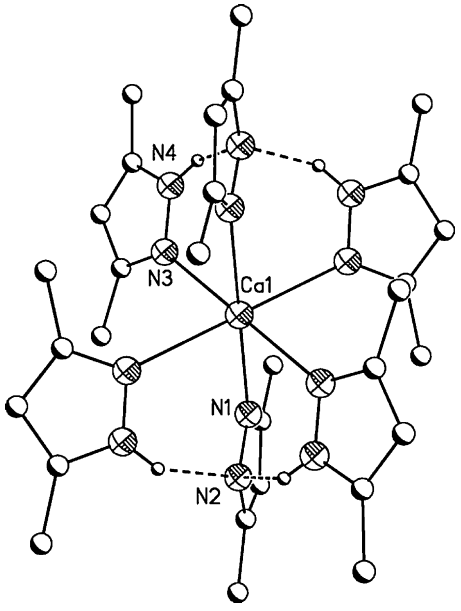

Fig. 17. Structure of $[Ca(Me_2pz)_2(Me_2pzH)_4]$ which demonstrates the hydrogen bonding embrace between coordinated neutral pyrazole and the anionic pyrazolate ligand. The complex $[Sr(Me_2pz)_2(Me_2pzH)_4]$ is isostructural and displays hydrogen bonding as well [148]. Hydrogen atoms not involved in agostic interactions removed for clarity. Agostic interactions shown as dashed lines.

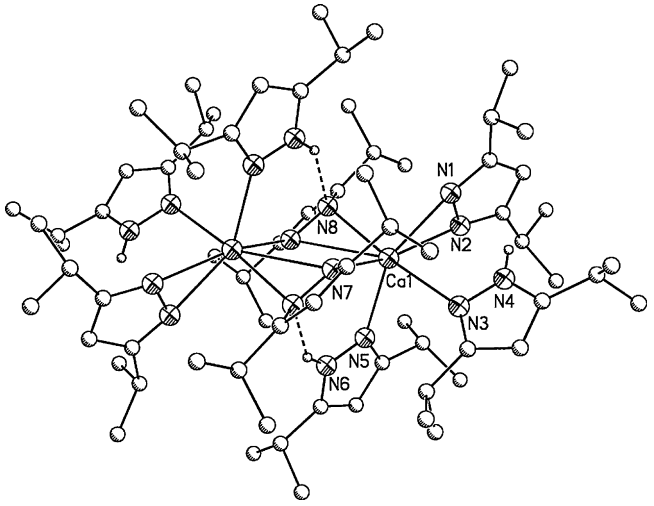

Fig. 19. Structure of $[\{Ca(^iPr_2pz)_2(^iPr_2pzH)_2\}_2]$. Hydrogen bonding between the terminal pyrazole ligand and the bridging pyrazolate ligand prevent higher ligand hapticity. Hydrogen atoms not involved in agostic interactions removed for clarity. Agostic interactions shown as dashed lines.

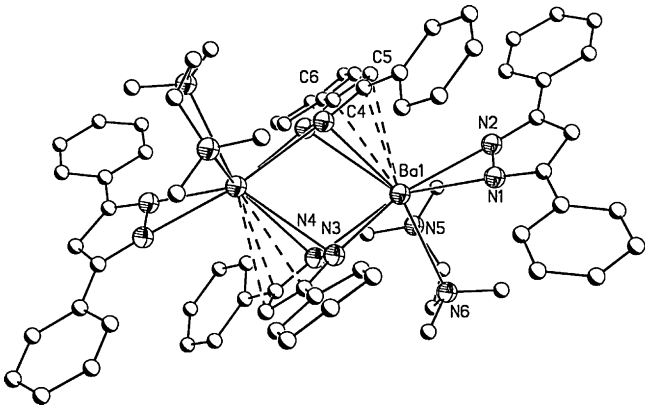

Fig. 20. Structure of [{Ba(Ph$_2$pz)$_2$(tmeda)}$_2$]·TMEDA. The bridging pyrazolates engage in π-bonding to the metal centers owing to the use of a smaller neutral donor [149]. Hydrogen atoms removed for clarity. M···C(π) interactions shown as dashed lines.

thallium M = Ca, with mercury M = Ca, Sr, Ba) [148], interestingly, all desolvate at room temperature. In all three, the Ph$_2$pz ligands adopt a transoid orientation with the four THF donors in equatorial positions. A complementary series of [M(Ph$_2$pz)$_2$(dme)$_n$] (M = Ca, Sr, n = 2; M = Ba, n = 3) displays the Ph$_2$pz ligands in a cisoid arrangement with the two DME donors capping the metal center [148]. The barium complex accommodates an extra DME donor.

Employing the bulkier bidentate donor TMEDA, the barium complexes [{Ba(Ph$_2$pz)$_2$(tmeda)}$_2$]·TMEDA and [Ba(Ph$_2$pz)$_2$(tmeda)$_2$]·TMEDA were obtained [149]. Both were synthesized via Route ii (Scheme 2) with the dimer forming from stoichiometric amounts of TMEDA; the monomer in the presence of excess amounts. The dimeric structure of [{Ba(Ph$_2$pz)$_2$(tmeda)}$_2$]·TMEDA (Fig. 20) is similar to [{Ba(Me$_2$pz)$_2$(pmdta)}$_2$] (see Fig. 18 above) and [{Ba(^{i}Pr$_2$pz)$_2$(py)$_3$}$_2$], however the reduced steric requirements and hapticity of the TMEDA donor as compared to PMDTA or three pyridine donors permits π-bonding of the bridging pyrazolates, giving a μ-η^5:η^2-binding mode (Table 12). The coordination of additional TMEDA led to the monomeric [Ba(Ph$_2$pz)$_2$(tmeda)$_2$]·TMEDA, which has η^2-coordinated pyrazolates in a transoid arrangement.

4.2.4. 3,5-Di-tert-butylpyrazolate (^{t}Bu$_2$pz)

The most commonly used pyrazolate is the bulky ^{t}Bu$_2$pz, with alkaline earth metal compounds exhibiting a wide range of nuclearity. Magnesium complexes include the donor-free [Mg$_2$(^{t}Bu$_2$pz)$_4$], in which the four-coordinate magnesium atoms are connected by two μ-η^1:η^1-bridging pyrazolates [156]. Each magnesium atom also has a terminal η^2-bound pyrazolate which lies nearly perpendicular to the plane of the bridging pyrazolates. A homoleptic monomeric magnesium species, [Mg(^{t}Bu$_2$pz)$_2$(^{t}Bu$_2$pzH)$_2$] was also reported. Curiously, the compound was obtained from a THF solution [152]. The solid-state structure reveals hydrogen bonding between the coordinated neutral ^{t}Bu$_2$pzH and anionic ^{t}Bu$_2$pz ligands (Table 12), similar to that observed in the heavier monomeric analogues [Ca(Me$_2$pz)$_2$(Me$_2$pzH)$_4$] and [Sr(Me$_2$pz)$_2$(Me$_2$pzH)$_4$] (see Fig. 17 above) [148]. Interestingly, the *iso*-propyl substituted analogues [{Mg(^{i}Pr$_2$pz)$_2$(^{i}Pr$_2$pzH)}$_2$] and [{Ca(^{i}Pr$_2$pz)$_2$(^{i}Pr$_2$pzH)$_2$}$_2$], which also exhibit pz···H···pz hydrogen bonding (see Fig. 19), form dimeric species even in the presence of excess neutral ligand. Detailed structural analysis reveals that the pz···H···pz hydrogen bonding in [{Mg(^{i}Pr$_2$pz)$_2$(^{i}Pr$_2$pzH)}$_2$] is shorter/stronger than in [Mg(^{t}Bu$_2$pz)$_2$(^{t}Bu$_2$pzH)$_2$], suggesting that hydrogen bonding has more influence than sterics over the resulting structure [151].

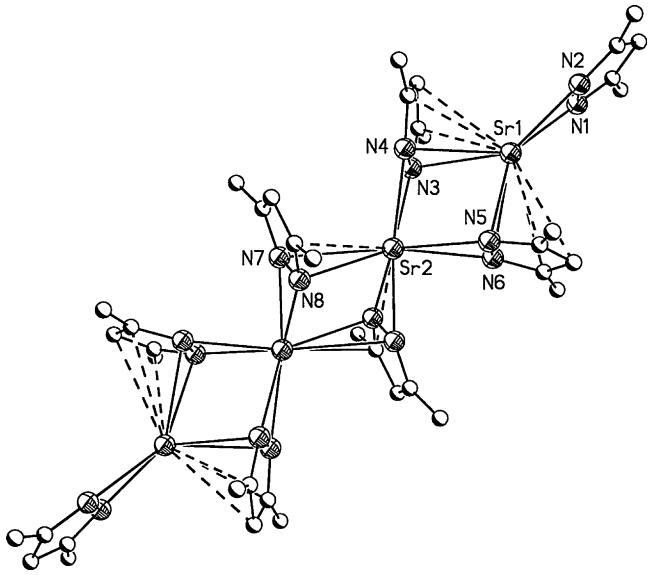

Fig. 21. Structure of [Sr$_4$(^{t}Bu$_2$pz)$_8$]. In the absence of neutral donors, π-bonding of the bridging pyrazolates satisfies coordinative saturation requirements, leading to oligomeric structures. Methyl groups on the *tert*-butyl groups are not shown for clarity [153]. Hydrogen atoms removed for clarity. M···C(π) interactions shown as dashed lines.

The heavier analogues are homoleptic oligomers of increasing chain length. The series of trimeric [Ca$_3$(^{t}Bu$_2$pz)$_6$], tetrameric [Sr$_4$(^{t}Bu$_2$pz)$_8$], and hexameric [Ba$_6$(^{t}Bu$_2$pz)$_{12}$] were synthesized via Route iii (Scheme 2) (Fig. 21) [153]. All are linear chains, with the metal ions bridged by pyrazolates in a variety of modes. An increase in points of contact is observed in the μ-η^2:η^2- and the μ-η^2:η^5-bridging pyrazolates of [Ca$_3$(^{t}Bu$_2$pz)$_6$] as compared to the μ-η^1:η^1-bridging found in [Mg$_2$(^{t}Bu$_2$pz)$_4$]. [Sr$_4$(^{t}Bu$_2$pz)$_8$] shows all bridging pyrazolates inclined and engaged in π-bonding and a M···C interaction of 3.22(1) Å, whereas the hexameric [Ba$_6$(^{t}Bu$_2$pz)$_{12}$] is a dimer of trinuclear units, with three unique barium centers with the bonding modes μ-η^2:η^2-, μ-η^2:η^4-, and μ-η^2:η^5-types (Table 12).

The ^{t}Bu$_2$pz complexes have been reported with a variety of donors, namely THF, pyridine, TMEDA, PMDTA, triglyme, and tetraglyme. In addition, some mixed-ligand species containing the ^{t}Bu$_2$pz ligand have also been reported. The THF adducts [Mg$_2$(^{t}Bu$_2$pz)$_4$(thf)$_2$], [Ca(^{t}Bu$_2$pz)$_2$(thf)$_2$] and [{M(^{t}Bu$_2$pz)$_2$(thf)}$_2$] (M = Ca, Sr, Ba), were obtained by a combination of synthetic routes including Route i, M = Mg, Ca, Route ii, M = Sr, Ba (Scheme 2), and by dissolving the homoleptic species in THF (Mg, Ca, Sr, Ba) [147,154,156]. Among the dimeric species, the bridging pyrazolates bind in modes of increasing π-contribution as metal size increases with μ-η^1:η^1 for [Mg$_2$(^{t}Bu$_2$pz)$_4$(thf)$_2$], μ-η^2:η^2 in [{Ca(^{t}Bu$_2$pz)$_2$(thf)}$_2$], and μ-η^5:η^2 in [{Sr(^{t}Bu$_2$pz)$_2$(thf)}$_2$] and [{Ba(^{t}Bu$_2$pz)$_2$(thf)$_2$}$_2$] (Table 12). All contain a terminal η^2-bound pyrazolate on each metal center. The larger Ba requires two THF molecules to attain steric saturation, while Sr achieves this with one THF molecule and close M···H–C contacts involving a *tert*-butyl group as well as an α-hydrogen on the coordinated THF molecule with a value of 2.937 Å for both agostic interactions (Fig. 22).

Employing the multidentate triglyme and tetraglyme co-ligands affords M(^{t}Bu$_2$pz)$_2$(triglyme) and M(^{t}Bu$_2$pz)$_2$(tetraglyme) (M = Ca, Sr, Ba) through Routes i and viii (Scheme 2) [147,157]. Similarly, the nitrogen-based neutral donors afforded the monomeric Mg(^{t}Bu$_2$pz)$_2$(tmeda), Ca(^{t}Bu$_2$pz)$_2$(py)$_3$, Ca(^{t}Bu$_2$pz)$_2$(tmeda), Ca(^{t}Bu$_2$pz)$_2$(pmdta), and Sr(^{t}Bu$_2$pz)$_2$(pmdta) [147,156,157], each with two terminal η^2-bound pyrazolate ligands.

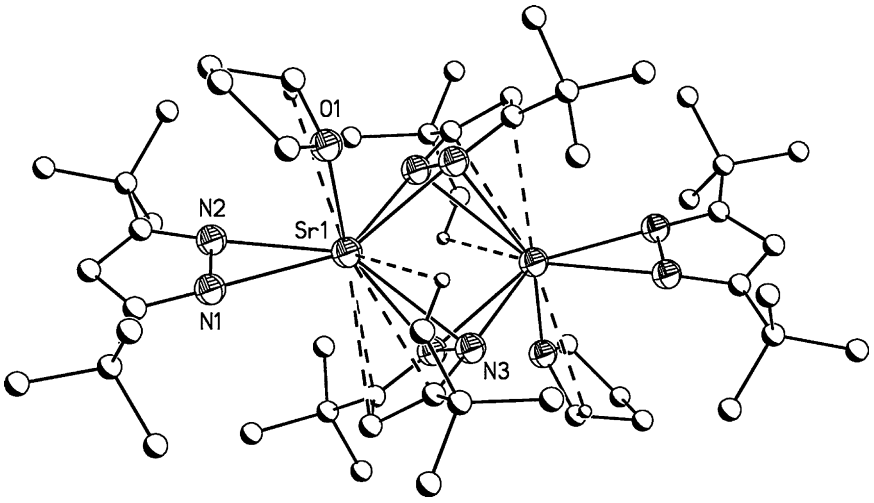

Fig. 22. Structure of $[\{Sr(^tBu_2pz)_2(thf)\}_2]$. The hydrogen atoms not involved in agostic interactions have been omitted for clarity [154]. Secondary interactions shown as dashed lines.

The mixed-ligand dimeric complexes$[Ca_2(^tBu_2pz)_3(L^{tBu})]$, $[\{Sr(^tBu_2pz)(L^{tBu})\}_2]$, and $[\{Ba(^tBu_2pz)(L^{tBu})\}_2]$ bearing the β-diketiminate ligand N-*tert*-butyl-4-(*tert*-butylimino)-2-penten-2-amine ($L^{tBu}H$) were achieved via Route viii (Scheme 2) [155]. The bridging pyrazolates engage in μ-η^5:η^2- and μ-η^2:η^2-binding (Table 12). The terminal ligands include η^2-pyrazolate and η^5-β-diketimine. Solution studies suggest that ligand rearrangement equilibria lie towards the formation of the mixed-ligand species due to entropic resistance to forming the oligomeric species, $[Ca_3(^tBu_2pz)_6]$, $[Sr_4(^tBu_2pz)_8]$, and $[Ba_6(^tBu_2pz)_{12}]$.

4.3. Asymmetrically substituted pyrazolate complexes

With the growing body of structural evidence of alkaline earth metal pyrazolates, it is becoming clear that factors beyond simple sterics are controlling the coordination chemistry of these compounds. Asymmetrically substituted pyrazolate ligands were studied to better understand factors such as solvation vs. ligation, agostic interactions, and π-bonding. The asymmetrically substituted pyrazolate complexes, all with barium, include $[\{Ba(Phpz)_2(pmdta)\}_2]$, $[\{Ba(^tBupz)_2(pmdta)\}_2]$, and $[\{Ba(MePhpz)_2(tmeda)\}_2]$ as well as the polymeric $[\{Ba(^tBupz)_2(NH_3)_2\}_n]$ [149].

The effects of ligand substitution can be seen by comparing the asymmetrically substituted $[\{Ba(Phpz)_2(pmdta)\}_2]$ and $[\{Ba(^tBupz)_2(pmdta)\}_2]$ (Fig. 23) with the symmetrically substituted $[\{Ba(Me_2pz)_2(pmdta)\}_2]$ (see Fig. 18 above). A general dimeric structure is observed for each complex, with two pyrazolate ligands bridging the barium ions and an η^2-bound terminal pyrazolate as well as a tridentate PMDTA donor on each barium ion. This arrangement leaves a portion of the metal coordination sphere exposed, and each of the complexes fills it differently: agostic interactions from a PMDTA methyl group in $[\{Ba(Phpz)_2(pmdta)\}_2]$, π-bonding from the bridging pyrazolates in $[\{Ba(^tBupz)_2(pmdta)\}_2]$, and twisting of the bridging pyrazolates in $[\{Ba(Me_2pz)_2(pmdta)\}_2]$.

The effects of the neutral donor may at first seem rather straightforward. For example, an increase in donor size and hapticity reduces the nuclearity along the series $[Ba_6(^tBu_2pz)_{12}]$, $[\{Ba(^tBu_2pz)_2(thf)_2\}_2]$, $Ba(^tBu_2pz)_2$(triglyme) and $Ba(^tBu_2pz)_2$(tetraglyme) [153,154,157]. However, non-covalent interactions become important in the case of $[\{Ba(^tBupz)_2(NH_3)_2\}_n]$ when compared to $[\{Ba(^tBupz)_2(pmdta)\}_2]$. The smaller coordinative and steric requirement of two ammonia donors, as compared to PMDTA, gives rise to increased π-interactions and hydrogen bonding of an ammonia–hydrogen atom to the uncoordinated nitrogen atom of an η^1-bound

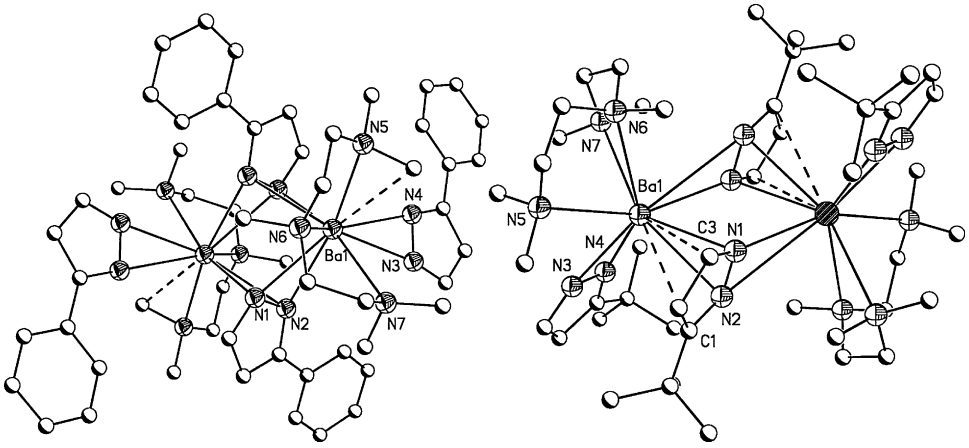

Fig. 23. Structures of $[\{Ba(Phpz)_2(pmdta)\}_2]$ and $[\{Ba(^tBupz)_2(pmdta)\}_2]$. Hydrogen atoms and some PMDTA methyl groups have been removed for clarity [149]. Agostic and M···C(π) interactions shown as dashed lines.

pyrazolate in [{Ba(^{t}Bupz)$_2$(NH$_3$)$_2$}$_n$]. The tendency towards π-bonding and/or aggregation increases with decreasing neutral donor size, as is observed for the bidentate TMEDA complexes [{Ba(MePhpz)$_2$(tmeda)}$_2$] and [{Ba(Ph$_2$pz)$_2$(tmeda)}$_2$]·TMEDA, which contain μ-η^2:η^5-bridging pyrazolates. The larger tridentate neutral donor PMDTA is found in [{Ba(Phpz)$_2$(pmdta)}$_2$], and prevents π-bonding, even though the steric bulk of the ligands is less.

4.4. Applications

Thermogravimetric analysis (TGA) and sublimation studies have been carried out on a number of the above compounds to evaluate their usefulness as CVD precursors. Of the series [{Mg(^{t}Bu$_2$pz)$_2$}$_2$], [{Mg(^{t}Bu$_2$pz)$_2$(thf)}$_2$], and [Mg(^{t}Bu$_2$pz)$_2$(tmeda)], only the homoleptic species sublimed intact (150 °C, 0.1 Torr). The others showed evidence of partial or complete loss of neutral donor prior to sublimation [156].

The loss of neutral donor was especially problematic for the heavier alkaline earth metal complexes. All of the compounds in the series of dimers [{Ca(^{t}Bu$_2$pz)$_2$(thf)}$_2$], [{Sr(^{t}Bu$_2$pz)$_2$(thf)}$_2$], and [{Ba(^{t}Bu$_2$pz)$_2$(thf)$_2$}$_2$] showed loss of coordinated THF prior to 150 °C [154]. Replacement of THF with other neutral donors did not change this outcome as the complexes Ca(^{t}Bu$_2$pz)$_2$(L)$_x$ (where L = pyr, x = 3; L = TMEDA, PMDTA and tetraglyme, x = 1) as well as Ca(Me$_2$pz)$_2$(L) (where L = PMDTA, triglyme and tetraglyme) decomposed prior to sublimation. The triglyme complex Ca(^{t}Bu$_2$pz)$_2$(triglyme) sublimed at 160 °C but also showed decomposition through loss of triglyme during the process [147]. A later report of the corresponding strontium and barium complexes [M(^{t}Bu$_2$pz)$_2$(L)] (where M = Sr and L = tetraglyme, triglyme, PMDTA; M = Ba and L = tetraglyme and triglyme) also showed that the complexes decomposed upon heating under vacuum (130–150 °C, 0.05 Torr) through loss of neutral ligand and pyrazole [157].

Interestingly, the homoleptic complexes of the heavier analogues, [Ca$_3$(^{t}Bu$_2$pz)$_6$], [Sr$_4$(^{t}Bu$_2$pz)$_8$], and [Ba$_6$(^{t}Bu$_2$pz)$_{12}$] did not sublime intact, which was noteworthy given that they were initially prepared and crystallized in sealed tubes in which they sublimed intact. Clearly, the dynamic vacuum (sublimation studies) or ambient pressures (in the TGA) used during analysis affects the stability of these complexes during vapor transport. These results indicate that heavy alkaline earth pyrazolate complexes, especially those containing neutral donors, are not suitable for applications as CVD precursors.

5. Pyrrolates

5.1. Pyrrolate ligand system

The pyrrolato ligand is capable of binding through the nitrogen in a σ-fashion or through the π-electrons of the five-membered ring. Theoretical calculations of the interactions between alkaline earth metals and the pyrrolate anion indicate that the mode of binding depends on metal size, with beryllium derivatives favoring σ–N-bonding, the calcium derivatives favoring π-bonding, and magnesium derivatives showing similar propensity for both [158]. The pyrrolate complexes of the alkaline earth metals reviewed here illustrate how substituents also impact coordination mode.

5.2. Pyrrole complexes

The most prominent pyrrole derivatives are based either on substituted pyrrolato complexes of the form [M(pyr*)$_2$(thf)] (where M = Ca, Sr, and pyr* = 2,5-di-*tert*-butylpyrrolate) or pyrrolato ligands with a linker arm, (CH$_3$)$_2$NCH$_2$–, which provides intramolecular stabilization in the monomeric complexes, [Ca(2-DMAMP)$_2$(donor)$_x$] (where 2-DMAMP = 2-(dimethylaminomethyl)pyrrole and donor = THF, pyr, x = 2; DME, TMEDA, x = 1) [159,160]. The calcium complexes of 2-DMAMP exhibit 6-coordinate metal centers, with the THF and pyridine adducts displaying *trans*-oriented ligands and donors and the DME and TMEDA adducts displaying *cis*-oriented ligands (Fig. 24). Unlike the π-bonded pyr* complexes of calcium, the presence of the linker arm in the 2-DMAMP complexes forces σ–N-bonding of the pyrrole nitrogen. Thermogravimetric analysis (TGA) studies of the four calcium complexes showed complex decomposition patterns for the ether-containing complexes, while the TMEDA adduct showed a cleaner TGA pattern but with a significant amount of residue remaining at 450 °C, indicating potential decomposition as well.

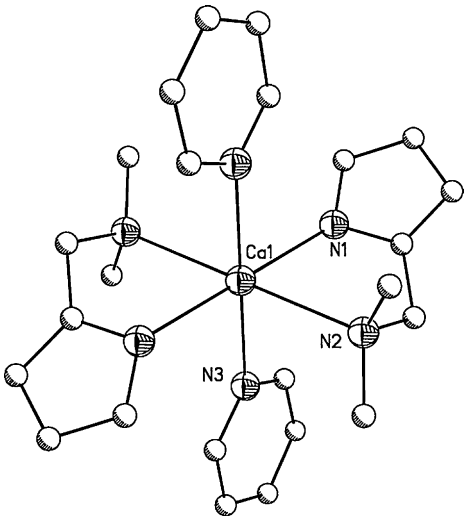

Fig. 24. Structure of [Ca(2-DMAMP)$_2$(pyridine)$_2$] [160]. Hydrogen atoms removed for clarity.

6. Triazolates and tetrazolates

6.1. Triazolates and tetrazolates ligand system

The triazolate ligand is of interest due to its ability to bridge metal centers in a variety of coordination modes. As such, a substituted triazolate ligand has appeared in an investigation of polynuclear magnesium species (Fig. 25).

Complexes of tetrazolate ligands are often sought as high energy density materials for applications of propulsion and explosion. A variety of substitution patterns are now possible, and tetrazolate ligands have appeared in complexes of alkaline earth metals in a number of recent publications, which are reviewed here (Fig. 25b). Alkaline earth metal pentazolate complexes have been the subject of theoretical investigations, but are not included in this review [161].

6.2. A triazolate complex

A μ-$_4$-oxo tetranuclear magnesium compound, [Mg$_4$(μ$_4$-oxo)(μ-triazolate)$_6$] (where triazolate = 3,5-^{i}Pr$_2$-1,2,4-triazolate)was obtained by Route i (Scheme 2) with an undetermined oxygen source [152]. The four magnesium atoms are centered around a μ$_4$-oxo-species, and are further bridged by six μ-η^1:η^1 triazolate ligands (Fig. 26).

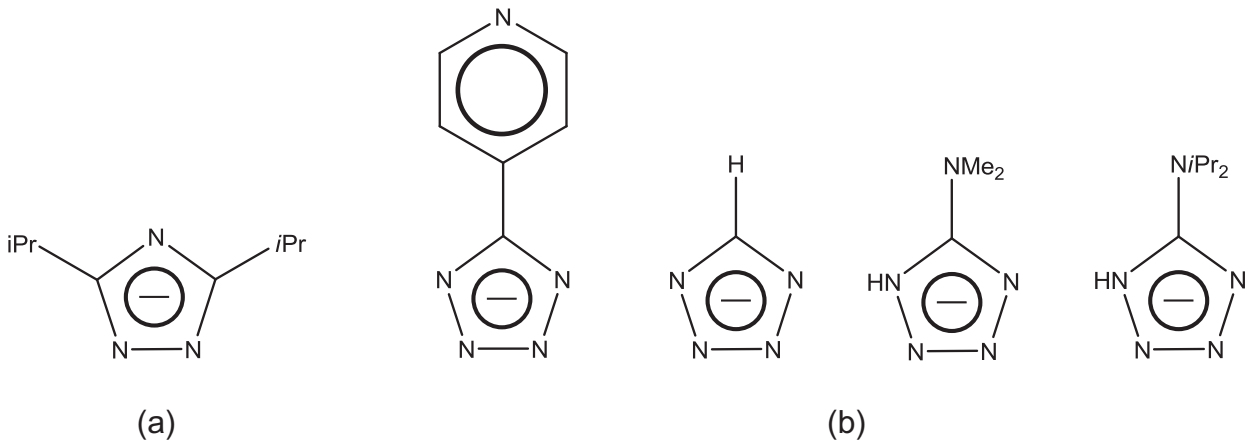

Fig. 25. (a) The 3,5-$^{i}Pr_2$-1,2,4-triazolate ligand used in investigations of polynuclear magnesium complexes. (b) A variety of substitution patterns of the tetrazolate ligand have been found in complexes of alkaline earth metals including 5-(4-pyridyl)tetrazolate anion, 1,2,3,4-tetrazolate, dimethylaminotetrazolate and diisopropylaminotetrazolate.

6.3. Tetrazolate complexes

A pyridine derivative of the tetrazolate ligand, 5-(4-pyridyl)tetrazolate anion, $(4\text{-PTZ})^{-}$, appears in the chain structure $[Ca_{1.5}((4\text{-PTZ})_2H)(N_3)_2(H_2O)_5](H_2O)_{0.3}$, which was obtained via reaction of 4-cyanopyridine and $Ca(N_3)_2$ [162]. Interestingly, the tetrazolate ligand in this complex is protonated, and is therefore zwitterionic. A three-dimensional network structure is the result of extensive hydrogen bonding between water molecules and the nitrogen atoms of the tetrazolate ligands.

An unsubstituted tetrazolate ligand is found in the dimeric strontium tetrazolate complex, $Sr_2(1,2,3,4\text{-tetrazolate})_4{\cdot}5H_2O$, which was synthesized via reaction of the protonated tetrazole, 1*H*-1,2,3,4-tetrazole and $Sr(OH)_2{\cdot}8H_2O$ [163]. The two strontium centers are bridged by two water molecules and two μ-η^1:η^1-tetrazolate ligands.

Two tetrazolate complexes of barium, [Ba(tetrazolate)$_2$(18-crown-6)] (where tetrazolate = dimethylaminotetrazolate ($CN_4(NMe_2)$) and diisopropylaminotetrazolate ($CN_4(N^{i}Pr_2)$)) were synthesized via Route viii (Scheme 2) in the presence of 18-crown-6 [164] (Fig. 27). Both structures show transoid-oriented tetrazolates with 18-crown-6 in the equatorial position. While the $CN_4(NMe_2)$ ligands adopt 1,2-η^2-coordination, the $CN_4(N^{i}Pr_2)$ ligands are 2,3-η^2-bound and bend towards the 18-crown-6 due to lone pair donation towards antibonding orbitals on the crown ether. Multiple N···H–C interactions in each compound ($CN_4(NMe_2)$ = 2.442–2.889, $CN_4(NiPr_2)$ = 2.422 –2.862 Å) add thermodynamic stability to the complex.

Finally, the barium tetrazolate salt [{Ba(HBTA)$_2{\cdot}4H_2O$}$_2$] (where HBTA = 5-(tetrazol-5-ylamino)tetrazolate) was synthesized and used for subsequent reactions with nitrogen rich cations to form high energy salts [165]. The HBTA^{-} anion is deprotonated H_2BTA,

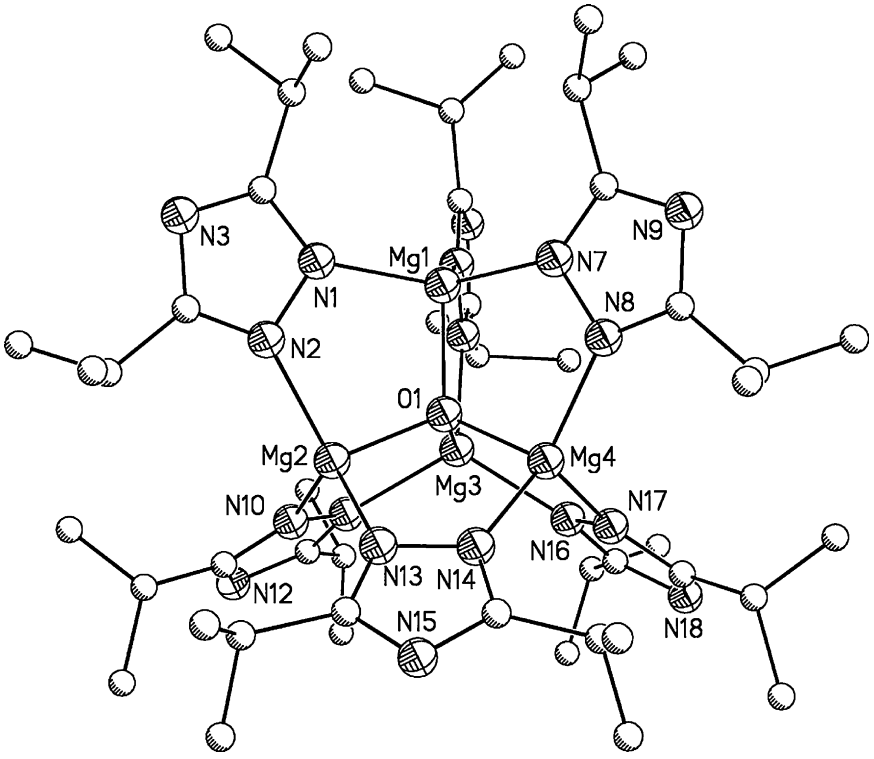

Fig. 26. Structure of [Mg_4(μ_4-oxo)(μ-triaz)$_6$]. Bond angle analysis indicated that ionic bonding forces were primarily responsible for the structure observed. Hydrogen atoms removed for clarity.

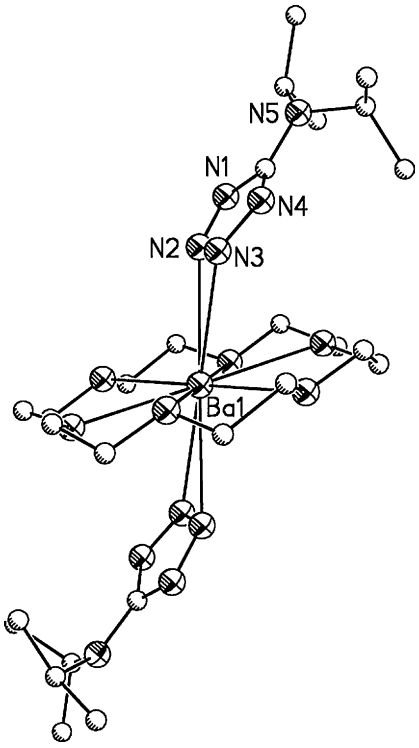

Fig. 27. Structure of $[Ba(CN_4(NiPr_2))_2(18\text{-crown-}6)]$. Hydrogen atoms removed for clarity.

which is an amine substituted with two tetrazole groups (Fig. 28). The salt, $Ba(HBTA)_2{\cdot}4H_2O$, was synthesized by reacting barium hydroxide with H_2BTA. The dimeric structure displays two barium atoms bridged by two μ-η^1:η^1 tetrazolate ligands and two water molecules.

7. Poly(pyrazolyl)borates and their derivatives

7.1. Poly(pyrazolyl)borate ligand system and their derivatives

In addition to acting as independent ligands, the azoles are also found as parts of larger, polydentate ligands. Most notable is the "scorpionate", or hydrotris(pyrazol-1-yl)borate (Tp) ligand, pioneered by Trofimenko [166]. Alkaline earth metal complexes of Tp and its derivatives have been known since the 1990s and were reviewed by Trofimenko in 1999 [167]. A more recent review by Chisholm focused on alkaline earth metal complexes of Tp and its derivatives that were developed for polymerization catalysts [168]. Here, we provide only a brief overview of the different ligand types and the main characteristics of the relevant complexes that have not previously been reviewed. Interest in these compounds arises from their applications in atomic layer deposition (ALD) as precursors for electronic materials, and as catalysts and bioorganometallic applications [150,169–171]. As multiple recent reviews are available on the topic, the following discussion will be brief.

7.2. Poly(pyrazolyl)borate complexes

The most common poly(pyrazolyl)borate complexes consist of a BH_n unit bridging two or three pyrazolates which are themselves bridged by a metal ion (Fig. 29). The dihydrobis(pyrazol-1-yl)borate (Bp) ligands are bidentate and typically coordinate to the metal in a κ^2-N,N′-binding mode with additional weak interactions between one of the boron-bound hydrogen atoms and the metal. The hydrotris(pyrazol-1-yl)borate (Tp) ligands are tridentate and typically coordinate to the metal center in a κ^3-N,N′,N″-binding mode. The boron-bound hydrogen typically does not interact with the metal. Both Bp and Tp are monoanionic ligands.

Alkaline earth metal complexes of these ligands are notable for improved stability against hydrolysis and oxidation. In general, the Tp complexes are more stable than Bp complexes having one fewer B–H site for reactions to occur. Multiple "generations" of the Tp ligands have been developed as different substitution patterns have been explored. Tp ligands with pyrazole rings bearing no substituents are considered first generation and are denoted as simply "Tp". Second generation Tp ligands have substituents in the 3- and 5-positions of the pyrazole, which allows for changes in electronic properties as well as sterics near the metal ion and the B–H group, respectively (Fig. 29). The identity and number of the substituents is denoted in superscript (Tp^{Rn}). Many examples of second generation Tp ligands and their complexes are known, owing to the ease with which the parent Tp ligands can be prepared. Lesser known are the third generation Tp ligands in which an alkyl or aryl group replaces the boron-bound hydrogen. Fourth generation scorpionates have very recently appeared in the literature (Fig. 29).

7.2.1. Dihydrobis(pyrazolyl)borate (Bp) complexes

The competition between solvent coordination and metal stabilization through M···H–B interaction is illustrated by the three magnesium complexes $[Mg_2(Bp)_2Cl_2(thf)_3]$, $[Mg(Bp)_2(thf)]$, and $[Mg(Bp)_2(thf)_2]$ [172]. In $[Mg_2(Bp)_2Cl_2(thf)_3]$ and $[Mg(Bp)_2(thf)_2]$ the coordination of solvent THF molecules precludes the need for M···H–B interactions resulting in κ^2-N,N′-coordination of the Bp ligand. In contrast, $[Mg(Bp)_2(thf)]$ has fewer coordinated THF molecules, so a weak Mg···H–B interaction takes place, giving rise to a κ^3-N,N′,H-coordinated Bp ligand.

The larger heavier alkaline earth metals typically display M···H–B interactions, as seen in the series of monomeric complexes $[M(Bp^{tBu2})_2(thf)_x]$ (M = Ca, Sr, Ba, $x = 0$; and M = Ba, $x = 1$; Bp^{tBu2} = 3,5-di-*tert*-butyl(pyrazolyl)borate) [173]. The crystal structures of $[Sr(Bp^{tBu2})_2]$, $[Ba(Bp^{tBu2})_2(thf)]$ and $[Ba(Bp^{tBu2})_2]$ display similar structural features, with each metal ion coordinated by two Bp^{tBu2} in a κ^3-N,N,H-binding mode. Also, ligand distortions, quantified by the M-N-N-B torsion angle, are caused by repulsions between bulky *tert*-butyl groups in the 3-position of each pyrazole. Volatility and decomposition studies indicate that these

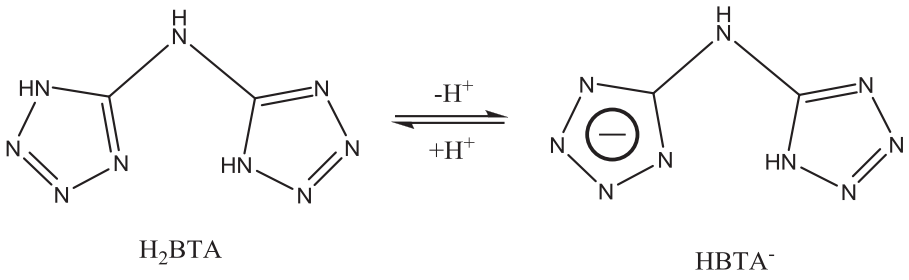

Fig. 28. The $HBTA^-$ anion found in $Ba(HBTA)_2{\cdot}4H_2O$ [165].

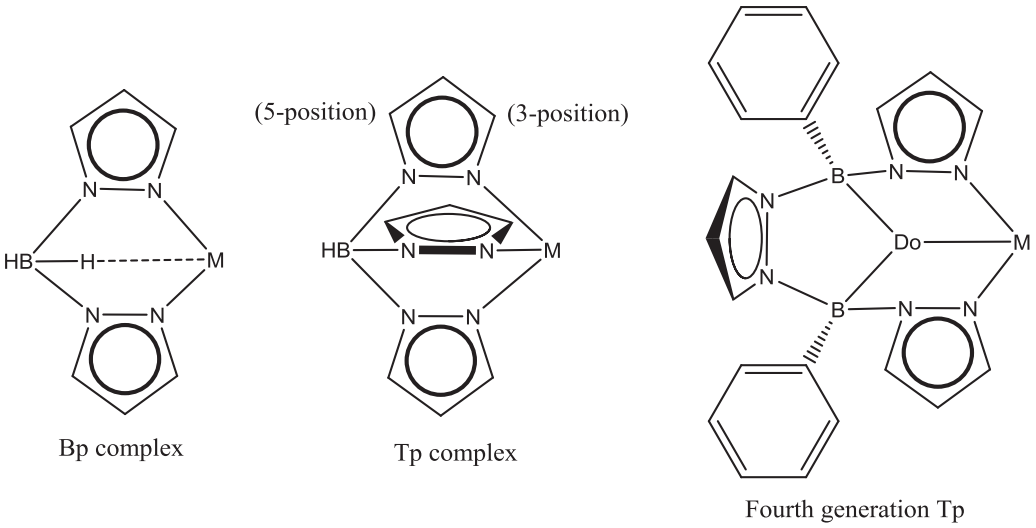

Fig. 29. General structures of bis(pyrazolyl)borate (Bp), which typically bind in a κ^3-N,N,H-fashion; tris(pyrazolyl)borate (Tp), where second generation Tp ligands are substituted in the 3- and 5-positions; third generation Tp ligands are substituted with an alkyl or aryl group on the boron in place of the hydrogen (not shown). Recently coined "fourth generation" scorpionates include a second boron atom, donor (Do) atoms such as nitrogen or oxygen, and a wider bite angle.

compounds are more stable than many known Group II CVD precursors, but they were less thermally stable than the corresponding Tp complexes described below [150,174].

7.2.2. Hydrotris(pyrazolyl)borate (Tp) complexes

The hydrotris(pyrazolyl)borate (Tp) ligands and its derivatives typically bind in a κ^3-N,N′,N″-binding mode without any noncovalent interactions. Most of the alkaline earth metal complexes of the Tp ligand class that have been previously reviewed follow this general trend [167,168,175].

The series of second generation Tp ligand complexes $[M(Tp^{R2})_2]$ (where M = Ca, Sr, Ba; R = 3,5-diethyl-; 3,5-di-*n*-propyl-) exhibit good volatility and high thermal stability due to the presence of bulky substituents [150]. In general, the complexes are monomeric with two κ^3-N,N′,N″-bound Tp ligands. The role of secondary interactions in these structures is minimal, however steric interactions between ligands were believed to force a "linear" arrangement, with boron–metal–boron bond angles of 180°, in complexes such as $Ca(Tp^{Et2})_2$ (Fig. 30a). This general linear arrangement is in contrast to one member of the series, $Ba(Tp^{Et2})_2$, which has two κ^3-N,N′,N″-bound Tp^{Et2} ligands arranged in a "bent" fashion, with a boron–metal–boron angle of 165.1(1)° (Fig. 30b). It is presumed that the larger coordination sphere of the barium ion allows this distortion from ideal geometry.

Instead of the usual κ^3-N,N′,N″-binding mode, the unsubstituted dimeric $[BaTp_2]_2$ displays metal–π bonding of the bridging Tp ligands [150] (Fig. 31). One pyrazole is η^5-bound to a barium ion, (Table 12) while the same pyrazole is η^1-bound to the other barium ion through the nitrogen atom. The remaining two pyrazole moieties bridge the metal centers in a Ba-(η^1-pz)-B-(η^1-pz)-Ba mode. Each barium center is terminally bound by a κ^3-N,N′,N″-Tp ligand.

Application studies of these complexes as ALD precursors are promising, as all of the complexes in the series $[M(Tp^{R2})_2]$ (M = Ca, Sr, Ba; R = Et, ^{n}Pr), with the exception of $Ca(Tp^{Et2})_2$, sublime as liquids. All demonstrate high thermal stability – the solid barium complexes decompose ~375 °C, the solid calcium and strontium complexes decompose >400 °C. Thermal gravimetric analysis (TGA) studies show low residue (ranging from 0.1 to 5.5%). Sublimation

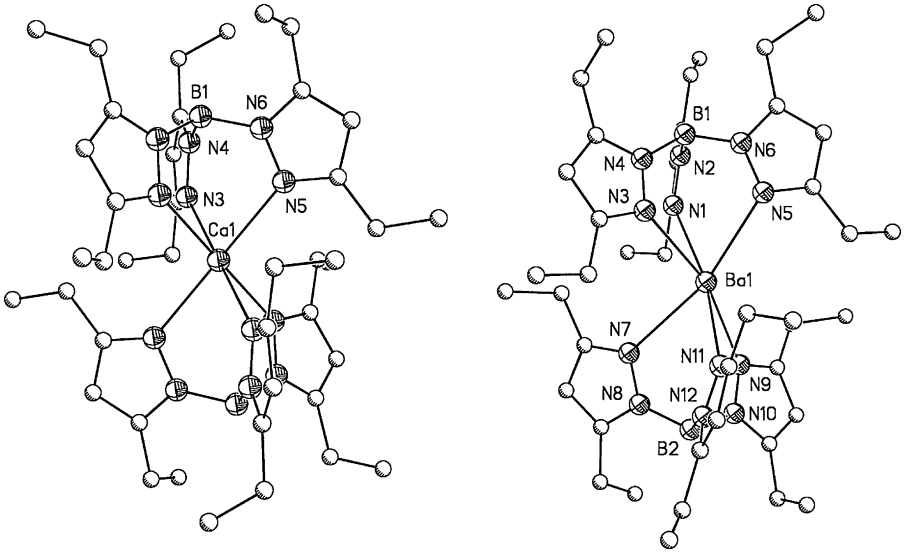

Fig. 30. Structures of (a) $Ca(Tp^{Et2})_2$ showing a "linear" arrangement of the ligands and (b) $[Ba(Tp^{Et2})_2]$ showing the "bent" arrangement of the ligands [150]. Hydrogen atoms removed for clarity.

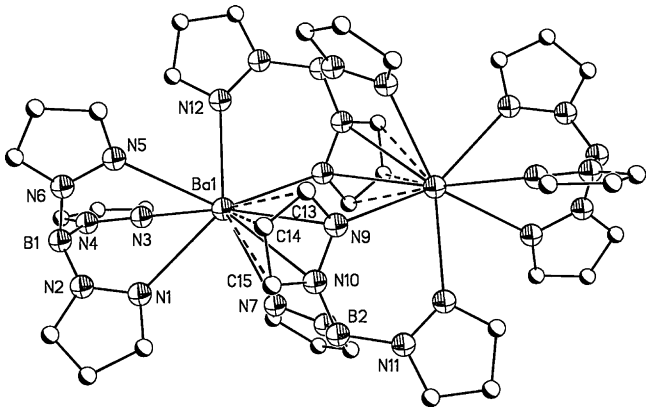

Fig. 31. Structure of $[Ba(Tp)_2]_2$. The flexibility of the Tp ligand allows the formation of a dimeric structure [150]. Hydrogen atoms removed for clarity. M···C(π) interactions shown as dashed lines.

recoveries were >99% for all but one of the series. A more detailed study of $Ba(Tp^{Et2})_2$ as a precursor in the ALD growth of BaB_2O_4 films was subsequently reported [174]. Not surprisingly, $Ba(Tp^{Et2})_2$ proved to be more thermally stable than existing precursors for Ba-containing thin film formation by CVD and ALD. Additionally, the precise control of B/Ba ratio (2:1) in the thin film could be attributed to the precursor composition.

Another second generation Tp complex, $Ca(Tp^{tBu})_2$, was isolated despite the bulky nature of the t-butyl substituents in the 3-position [176]. Structural data revealed one of the Tp^{tBu} ligands coordinating in an unusual κ^3-N,N,H-binding mode, in which one of the pyrazole rings does not bind to the metal center, and the boron-bound hydrogen coordinates in its place. The other Tp^{tBu} ligand coordinated in the typical κ^3-N,N′,N″-fashion, but with two pyrazoles tilted towards each other, which allowed coordination of the two pyrazoles from the first ligand.

Examples of third generation alkaline earth Tp complexes include magnesium complexes, in which the boron-bound hydrogen is replaced with a phenyl group [177]. Examples include the monomeric $(PhTp^{tBu})MgR$ (R = Me, Et; $PhTp^{tBu}$ = phenyl[tris(3-*t*-butylpyrazolyl)borate]) complexes, displaying approximately tetrahedral geometry, and a magnesium sandwich complex, $Mg(p\text{-}BrC_6H_4Tp)_2$ ($p\text{-}BrC_6H_4Tp$ = *para*-bromophenyl[tris(pyrazolyl)borate]), with a distorted octahedral environment of the magnesium atoms, similar to that reported for the first and second generation $MgTp_2$ complexes [171].

"Fourth generation" scorpionates have recently been presented by Wagner and coworkers [170]. Here the Tp ligand was modified to allow control over ligand field strength through the use of donor atoms other than nitrogen. In addition, the use of two boron atoms opens the bite angle to allow for meridional binding, as opposed to the more common facial coordination of traditional Tp ligands (Fig. 29). Among a set of main group and transition metal complexes reported were two fourth generation Tp monomeric magnesium complexes, $[Mg(Cl)(thf)_xL^1]$ and $[Mg(Cl)(thf)_2L^2]$, where $L^1 = [Ph(pz)B(\mu\text{-}N(Me))(\mu\text{-}pz)B(pz)Ph]^-$ and $L^2 = [Ph(pz)B(\mu\text{-}O)(\mu\text{-}pz)B(pz)Ph]^-$. In addition a dinuclear aggregate bridged by chlorine atoms $[L^1Mg(\mu\text{-}Cl)_2Mg(thf)L^1]$ was also synthesized. Structural analysis of $[Mg(Cl)(thf)_2L^2]$ reveals a facially coordinating L^2, while $[L^1Mg(\mu\text{-}Cl)_2Mg(thf)L^1]$ displays meridional coordination of L^1.

7.2.3. Hydrotris(triazolyl)borate complexes

Triazolyl derivatives of the traditional Tp ligand can lead to interesting electronic effects (Fig. 32). While most of the other compounds reported in this review are sensitive to air and moisture, $[M(HB(triazolyl)_3)_2(H_2O)_2]$,where M = Ca, Sr, were synthesized by

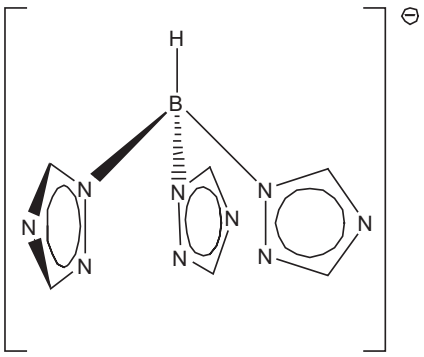

Fig. 32. The hydrotris(1,2,4-triazolyl)borate ligand, abbreviated $[HB(triazolyl)_3]^-$.

the aqueous reaction of $Ca(NO_3)_2$ or $SrCl_2$, respectively, with the potassium salt, $K(HB(triazolyl)_3)$ [178]. Attempts to form the magnesium and barium analogues by the same route were not successful. Structural analysis of $[Ca(HB(triazolyl)_3)_2(H_2O)_2]\cdot 2H_2O$ revealed a bending of the (HB(triazolyl)) ligands (B···M···B, 131.0°), reminiscent of $Ba(Tp^{Et2})_2$ [150]. However, the bending here is due to the coordination of two water molecules. The electronic effects of triazolyl can be observed in the longer Ca–N bond distances in $[Ca(HB(triazolyl)_3)_2(H_2O)_2]\cdot 2H_2O$ compared to the corresponding $CaTp_2$ complexes, suggesting that the triazolyl-based ligand has increased ionic interactions with the metal ion compared to the corresponding $CaTp_2$ complexes. The strontium complex, $[Sr(HB(triazolyl)_3)_2(H_2O)_2]\cdot 2H_2O$ was isostructural with the calcium complex, based on powder X-ray diffraction data.

7.3. Poly(pyrazolyl)methane complexes

Another derivative of the classic Tp ligand system is obtained by replacing the anionic BH^- group with CH, resulting in the neutral and isoelectric tris(pyrazolyl)methane ligand (Fig. 33a). The neutral tris(pyrazolyl)methane can be deprotonated at the C-bound hydrogen to give the tris(pyrazolyl)methanide anion (Fig. 33b). Methyl substituents in the 3- and 5-positions on each of the pyrazole rings give $\{HC(Me_2pz)_3\}$ and $\{C(Me_2pz)_3\}^-$ respectively, providing steric protection to both the coordinated metal and the carbanion. The alkaline earth metal complexes of poly(pyrazolyl)alkanes that have not previously been reviewed will be discussed [179,180].

The $\{HC(Me_2pz)_3\}$ and $\{C(Me_2pz)_3\}^-$ ligands afford the sandwich compound $[Mg\{C(Me_2pz)_3\}_2]$ and a variety of half-sandwich compounds including $[Mg\{C(Me_2pz)_3\}Ph(thf)]$

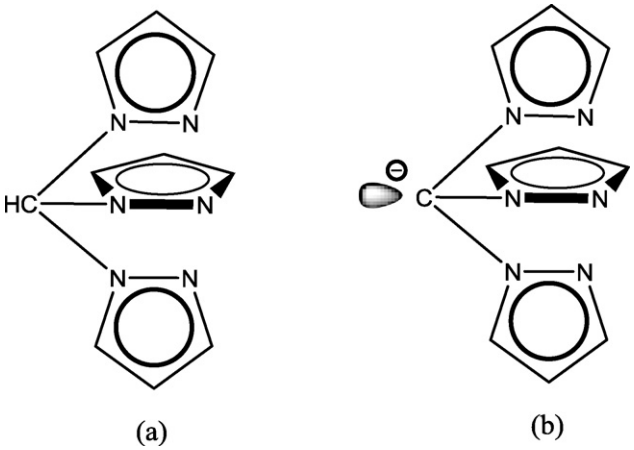

Fig. 33. (a) Tris(pyrazolyl)methane is neutral and (b) tris(pyrazolyl)methanide is anionic.

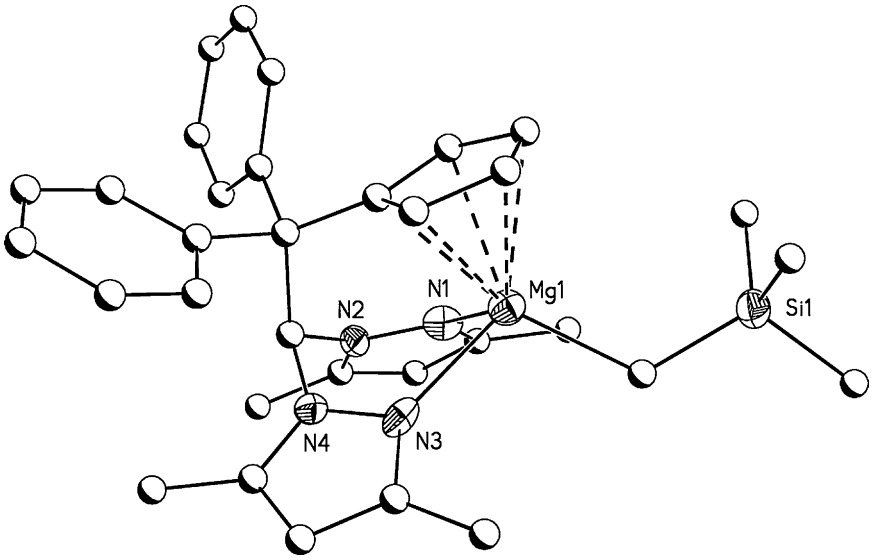

Fig. 34. Structure of [Mg(CH_2SiMe_3)(κ^2-μ^5-bpzcp)] [169]. Hydrogen atoms removed for clarity. M···C(π) interactions shown as dashed lines.

and [Mg{HC(Me_2pz)$_3$}Cl_2(thf)] [181], in addition to a charge separated species, [Mg{HC(Me_2pz)$_3$}$_2$][O_3SCF_3]$_2$. Notably [Mg{HC(Me_2pz)$_3$}Cl_2(thf)] is the first half-sandwich tris(pyrazolyl)methane complex of any Group II metal, while [Mg{C(Me_2pz)$_3$}$_2$] and [Mg{C(Me_2pz)$_3$}Ph(thf)] display the first Mg species to contain "naked" sp^3-hybridized carbanionic centers.

In a subsequent report, the {HC(Me_2pz)$_3$} ligand was reacted with a number of silyl amides: Mg[N($SiMe_3$)$_2$]$_2$, Mg[N($SiHMe_2$)$_2$]$_2$, and Ca[N($SiMe_3$)$_2$]$_2$(thf)$_2$, affording the heteroleptic Mg{C(Me_2pz)$_3$}{N($SiMe_3$)$_2$} at room temperature after 24 h with longer reaction time affording [Mg{C(Me_2pz)$_3$}$_2$] [182]. In the solid state Mg{C(Me_2pz)$_3$}{N($SiMe_3$)$_2$} exhibits a zwitterionic complex with a "free" pyramidal cation. Monitoring the reaction by VT NMR, at low temperatures, Mg{κ^2*N*-HC(Me_2pz)$_3$}{N($SiMe_3$)$_2$}$_2$ was identified using ROESY data; at temperatures above 0 °C, one of the two {N($SiMe_3$)$_2$} groups is eliminated affording Mg{κ^3*N*-C(Me_2pz)$_3$}{N($SiMe_3$)$_2$}. Similar results were found for the less bulky {N($SiHMe_2$)$_2$} ligand, leading to the isolation of the relatively stable intermediate Mg{κ^2*N*-HC(Me_2pz)$_3$}{N($SiHMe_2$)$_2$}$_2$. Formation of the analogous Mg{κ^3*N*-C(Me_2pz)$_3$}{N($SiHMe_2$)$_2$} product was only achieved by heating the solution at 70 °C for several hours. Further ^{1}H NMR studies using the deuterated analogue, Mg{κ^2*N*-DC(Me_2pz)$_3$}{N($SiHMe_2$)$_2$}$_2$, showed that C–H bond cleavage is the rate-determining step of the conversion between intermediate Mg{κ^2*N*-HC(Me_2pz)$_3$}{N($SiHMe_2$)$_2$}$_2$ and Mg{κ^3*N*-C(Me_2pz)$_3$}{N($SiHMe_2$)$_2$}. Finally, reactions of {HC(Me_2pz)$_3$} with Ca[N($SiMe_3$)$_2$]$_2$(thf)$_2$ yielded both the half-sandwich, [Ca{C(Me_2pz)$_3$}{N($SiMe_3$)$_2$}(thf)] and the sandwich [Ca{C(Me_2pz)$_3$}$_2$] complexes. Structural characterization of both showed that the former has distorted trigonal bipyramidal geometry, similar to that seen in the above mentioned [Mg{C(Me_2pz)$_3$}Ph(thf)]. The latter is the analogue of the above mentioned [Mg{C(Me_2pz)$_3$}$_2$].

Intentional incorporation of secondary interactions can be a strategy of ligand design, as shown with the incorporation of a cyclopentadienyl fragment into the poly(pyrazolyl)methane ligand system to develop initiators for ring-opening polymerization [169]. Among the complexes synthesized were a series of magnesium species of the formula [Mg(R)(κ^2-μ^5-bpzcp)] where R = Me, Et, ^{n}Bu, ^{t}Bu, CH_2SiMe_3, and CH_2Ph, and bpzcp = 2,2-bis(3,5-dimethylpyrazol-1-yl)-1,1-diphenylethylcyclopentadienyl (Fig. 34). NMR studies indicated that the two pyrazoles are equivalent and the –C_5H_4 fragment is μ^5-bound. Structural characterization of the ^{t}Bu and CH_2SiMe_3 derivatives revealed monomeric complexes with distorted tetrahedral coordination of the Mg-ion due to the κ^2-N,N-coordination of the scorpionate-portion and μ^5-coordination of the –C_5H_4 fragment.

8. Summary

The chemistry of nitrogen-based alkaline earth metal species has seen significant progress in the last decade, with the synthesis and characterization of a large array of compounds. Many of these compounds have applications in synthetic, polymer or materials chemistry, ensuring their continued development. An important design element in the further development of the target compounds is non-covalent interactions, whose significance is only now being recognized. Further development will recognize these interactions as a means to influence the structure and function of the target compounds.

Acknowledgements

The authors gratefully acknowledge support from the National Science Foundation (CHE 0753807), Syracuse University and the Le Moyne College Research and Development Committee.

References

[1] C. Elschenbroich, Organometallics, Wiley-VCH Verlag GmnH & Co, KGaA, Weinheim, 2006.
[2] J.S. Alexander, M.F. Zuniga, M.A. Guino-o, R.C. Hahn, K. Ruhlandt-Senge, The Encyclopedia of Inorganic Chemistry, Wiley, 2006, p. 116.
[3] R.D. Shannon, Acta Crystallogr. Sect. A: Found. Crystallogr. A32 (1976) 751.
[4] M. Mantina, A.C. Chamberlin, R. Valero, C.J. Cramer, D.G. Truhlar, J. Phys. Chem. A 113 (2009) 5806.
[5] A.L. Allred, E.G. Rochow, J. Inorg. Nucl. Chem. 5 (1958) 264.
[6] C. Lambert, P.v.R. Schleyer, Angew. Chem. 106 (1994) 1187.
[7] M. Westerhausen, Coord. Chem. Rev. 176 (1998) 157.
[8] S. Harder, Organometallics 21 (2002) 3782.
[9] H. Chen, R.A. Bartlett, H.V. Rasika Dias, M.M. Olmstead, P.P. Power, J. Am. Chem. Soc. 111 (1989) 4338.
[10] R.A. Bartlett, M.M. Olmstead, P.P. Power, Inorg. Chem. 33 (1994) 4800.
[11] M.F. Lappert, P.P. Power, A.R. Sanger, R.C. Srivastava, Metal and Metalloid Amides: Syntheses, Structures and Physical and Chemical Properties, Horwood-Wiley, Chichester, 1980.
[12] M.F. Lappert, A.V. Protchenko, P.P. Power, A.L. Seeber, Metal Amide Chemistry, Wiley, Chichester, 2009.
[13] M.F. Zuniga, G.B. Deacon, K. Ruhlandt-Senge, Chem. Eur. J. 13 (2007) 1921.
[14] M.F. Zuniga, G.B. Deacon, K. Ruhlandt-Senge, Inorg. Chem. 47 (2008) 4669.

[15] G.B. Deacon, P.C. Junk, G.J. Moxey, K. Ruhlandt-Senge, C.St. Prix, M.F. Zuniga, Chem. Eur. J. 15 (2009) 5503.
[16] W.D. Buchanan, D.G. Allis, K. Ruhlandt-Senge, Chem. Commun. 46 (2010) 4449.
[17] M. Brookhart, M.L.H. Green, J. Org. Chem. 250 (1983) 395.
[18] M. Gillett-Kunnath, W. Teng, W. Vargas, K. Ruhlandt-Senge, Inorg. Chem. 44 (2005) 4862.
[19] M. Gillett-Kunnath, J.G. MacLellan, C.M. Forsyth, P.C. Andrews, G.B. Deacon, K. Ruhlandt-Senge, Chem. Commun. 37 (2008) 4490.
[20] M. Westerhausen, W. Schwarz, Z. Anorg. Allg. Chem. 604 (1991) 127.
[21] M. Westerhausen, W. Schwarz, Z. Anorg. Allg. Chem. 606 (1991) 177.
[22] M. Westerhausen, W. Schwarz, Z. Anorg. Allg. Chem. 609 (1992) 39.
[23] B.A. Vaarstra, J.C. Huffman, W.E. Streib, K.G. Caulton, Inorg. Chem. 30 (1991) 121.
[24] M. Westerhausen, M. Hartmann, N. Makropoulous, B. Wieneke, M. Wieneke, W. Schwarz, D. Stalke, Z. Naturforsch. B: Chem. Sci. 53 (1998) 117.
[25] D.C. Bradley, M.B. Hursthouse, A.A. Ibrahim, A.M. Abdul, R. Motevalli, R. Moseler, H. Powell, J.D. Runnacles, A.C. Sullivan, Polyhedron 9 (1990) 2459.
[26] M. Westerhausen, Inorg. Chem. 30 (1991) 96.
[27] L.M. Engelhardt, B.S. Jolly, P.C. Junk, C.L. Raston, B.W. Skelton, A.H. White, Aust. J. Chem. 39 (1986) 1337.
[28] K.W. Henderson, J.F. Allan, A.R. Kennedy, J. Chem. Soc., Chem. Commun. (1997) 1149.
[29] J.M. Boncella, C.J. Coston, J.K. Cammack, Polyhedron 10 (1991) 769.
[30] R.L. Kuhlman, B.A. Vaarstra, K.G. Caulton, Inorg. Chem. 31 (1997) 8.
[31] G. Lessene, M. Bordeau, C. Biran, D. de Montauzon, J. Gerval, J. Electroanal. Chem. 490 (2000) 79.
[32] A.H. Clark, A. Haaland, J. Chem. Soc., Chem. Commun. (1970) 912.
[33] A.H. Clark, A. Haaland, Acta Chem. Scand. 24 (1970) 3024.
[34] H. Nöth, D. Schlosser, Inorg. Chem. 22 (1983) 2700.
[35] T.-Y. Her, C.-C. Chang, G.-H. Lee, S.-M. Peng, Y. Wang, J. Chin. Chem. Soc. 40 (1993) 315.
[36] F.G.N. Cloke, P.B. Hitchcock, M.F. Lappert, G.A. Lawless, B. Royo, Chem. Commun. (1991) 724.
[37] C. Eaborn, S.A. Hawkes, P.B. Hitchcock, J.D. Smith, J. Chem. Soc., Chem. Commun. (1997) 1961.
[38] M. Westerhausen, Trends Organomet. Chem. 2 (1997) 89.
[39] M. Westerhausen, J. Greul, H.-D. Hausen, W. Schwarz, Z. Anorg. Allg. Chem. 622 (1996) 1295.
[40] A.G.M. Barrett, M.R. Crimmin, M.S. Hill, G. Kociok-Kohn, D.J. MacDougall, M.F. Mahon, P.A. Procopiou, Organometallics 27 (2008) 3939.
[41] G.C. Forbes, A.R. Kennedy, R.E. Mulvey, P.J.A. Rodger, R.B. Rowlings, J. Chem. Soc., Dalton Trans. (2001) 1477.
[42] J.L. Sebestl, T.T. Nadasdi, M.J. Heeg, C.H. Winter, Inorg. Chem. 37 (1998) 1289.
[43] M. Arrowsmith, M.S. Hill, D.J. MacDougall, M.F. Mahon, Angew. Chem., Int. Ed. 48 (2009) 4013.
[44] J.S. Alexander, K. Ruhlandt-Senge, H. Hope, Organometallics 22 (2003) 4933.
[45] A.G. Avent, M.R. Crimmin, M.S. Hill, P.B. Hitchcock, Dalton Trans. (2005) 278.
[46] H. Phull, D. Alberti, I. Korobkov, S. Gambarotta, P.H.M. Budzelaar, Angew. Chem., Int. Ed. 45 (2006) 5331.
[47] M.R. Crimmin, A.G.M. Barrett, M.S. Hill, P.A. Procopiou, Org. Lett. 9 (1997) 331.
[48] A.G.M. Barrett, T.C. Boorman, M.R. Crimmin, M.S. Hill, G. Kociok-Kohn, P.A. Procopiou, Chem. Commun. (2008) 5206.
[49] A.G. Avent, M.R. Crimmin, M.S. Hill, P.B. Hitchcock, J. Organomet. Chem. 691 (2006) 1242.
[50] K.W. Henderson, W.J. Kerr, J.H. Moir, Tetrahedron 58 (2002) 4573.
[51] B.J. Wakefield, Organomagnesium Methods in Organic Synthesis, Academic Press, London, 1995.
[52] M.H. Chisholm, J.C. Gallucci, K. Phomphrai, Chem. Commun. (2003) 48.
[53] U. Wannagat, H. Kuckertz, Angew. Chem. 75 (1963) 95.
[54] V.U. Wannagat, H. Autzen, H. Kuckertz, H.-J. Wismar, Z. Anorg. Allg. Chem. 394 (1972) 254.
[55] T. Fjeldberg, R.A. Andersen, J. Mol. Struct. 125 (1984) 287.
[56] Z. Zhong, S. Schneiderbauer, P.J. Dijkstra, M. Westerhausen, J. Feijen, J. Polym. Environ. 9 (2001) 31.
[57] A. Yanagisawa, S. Habaue, H. Yamamoto, J. Am. Chem. Soc. 113 (1991) 8955.
[58] A. Yanagisawa, S. Habaue, K. Yasue, H. Yamamoto, J. Am. Chem. Soc. 116 (1994) 6130.
[59] S. Harder, F. Feil, K. Knoll, Angew. Chem. Int. Ed. 40 (2001) 4261.
[60] S. Harder, F. Feil, A. Weeber, Organometallics 20 (2001) 1044.
[61] M. Westerhausen, S. Scheneiderbauer, A.N. Kneifel, Y. Söltl, P. Mayer, H. Nöth, Z. Zhong, P.J. Dijkstra, J. Feijen, Eur. J. Inorg. Chem. (2003) 3432.
[62] D.J. Otway, W.S. Rees, Coord. Chem. Rev. 210 (2000) 279.
[63] C.H. Winter, J.L. Sebestl, M.J. Heeg, Mater. Res. Soc. Symp. Proc. 495 (1998) 147.
[64] J.S. Mathews, W.S. Rees, Adv. Inorg. Chem. 50 (2000) 173.
[65] Y. Tang, Z.L.N.A.L. Rheingold, R.A. Kemp, Organometallics 24 (2005) 836.
[66] Y. Tang, R.A. Kemp, Inorg. Chim. Acta 358 (2005) 2014.
[67] W. Vargas, U. Englich, K. Ruhlandt-Senge, Inorg. Chem. 41 (2002) 5602.
[68] A.R. Kennedy, R.E. Mulvey, J.H. Schulte, Acta Crystallogr. Sect. C: Cryst. Struct. Commun. 57 (2001) 1288.
[69] A. Torvisco, K. Ruhlandt-Senge, Chem. Eur. J., in preparation.
[70] A. Torvisco, K. Ruhlandt-Senge, Organometallics 30 (2011) 986.
[71] R.A. Bartlett, P.P. Power, J. Am. Chem. Soc. 109 (1987) 6509.
[72] P.B. Hitchcock, A.V. Khvostov, M.F. Lappert, A.V. Protchenko, J. Organomet. Chem. 647 (2002) 198.
[73] A. Torvisco, K. Decker, F. Uhlig, K. Ruhlandt-Senge, Inorg. Chem. 48 (2009) 11459.
[74] Y. Tang, L.N. Zakharov, A.L. Rheingold, R.A. Kemp, Inorg. Chim. Acta 359 (2006) 775.
[75] C. Koch, A. Malassa, C. Agthe, H. Görls, R. Biederman, H. Krautscheid, M. Westerhausen, Z. Anorg. Allg. Chem. 633 (2007) 375.
[76] B. Goldfuss, P.v.R. Schleyer, S. Handschuh, F. Hampel, W. Bauer, Organometallics 16 (1997) 5999.
[77] M. Gärtner, R. Fischer, J. Langer, H. Görls, D. Walther, M. Westerhausen, Inorg. Chem. 46 (2007) 5118.
[78] K.-C. Yang, C.-C. Chang, J.-Y. Huang, C.-C. Lin, G.-H. Lee, Y. Wang, M.Y. Chiang, J. Organomet. Chem. 648 (2002) 176.
[79] C. Glock, H. Görls, M. Westerhausen, Inorg. Chem. 48 (2009) 394.
[80] M. Gärtner, H. Görls, M. Westerhausen, Dalton Trans. (2008) 1574.
[81] W. Clegg, F.J. Craig, K.W. Henderson, A.R. Kennedy, R.E. Mulvey, P.A. O'Neil, D. Reed, Inorg. Chem. 36 (1997) 6238.
[82] M.M. Olmstead, W.J. Grigsby, D.R. Chacon, T. Hascall, P.P. Power, Inorg. Chim. Acta 251 (1996) 273.
[83] G.E. Coates, F. Glockling, J. Chem. Soc. (1954) 22.
[84] J.L. Atwood, G.D. Stucky, Chem. Commun. (1967) 1169.
[85] J.L. Atwood, G.D. Stucky, J. Am. Chem. Soc. 91 (1969) 4426.
[86] R. Juza, H. Schumacher, Z. Anorg. Allg. Chem. 324 (1963) 278.
[87] R. Juza, Angew. Chem. 76 (1964) 290.
[88] H. Jacobs, C. Hadenfeld, Z. Anorg. Allg. Chem. 418 (1975) 132.
[89] M. Kaupp, P.v.R. Schleyer, J. Am. Chem. Soc. 114 (1992) 491.
[90] G. Mösges, F. Hampel, M. Kauup, P.v.R. Schleyer, J. Am. Chem. Soc. (1992) 10880.
[91] M. Gärtner, H. Görls, M. Westerhausen, Inorg. Chem. 46 (2007) 7678.
[92] A. Torvisco, Thesis Dissertation, Syracuse University, Syracuse, NY 2010.
[93] M. Westerhausen, T. Bollwein, N. Makropoulous, H. Piotrowski, Inorg. Chem. 44 (2005) 6439.
[94] J.A. Rood, S.E. Hinman, B. Noll, K.W. Henderson, Eur. J. Inorg. Chem. (2008) 3935.
[95] A. Torvisco, K. Ruhlandt-Senge, Inorg. Chem., in preparation.
[96] A.R. Katritzky, I. Ghiviriga, P.J. Steel, D.C. Oniciu, J. Chem. Soc., Perkin Trans. 2 (1996) 443.
[97] P. Fischer, A. Fettig, Magn. Reson. Chem. 35 (1997) 839.
[98] B.K. Shull, D.E. Spielvogel, R. Gopalaswamy, S. Sankar, P.D. Boyle, G. Head, K. Devito, J. Chem. Soc., Perkin Trans. 2 (2000) 557.
[99] H.S. Gutowsky, C.H. Holm, J. Chem. Phys. 25 (1956) 1228.
[100] J.B. Lambert, L. Lin, Magn. Reson. Chem. 39 (2001) 714.
[101] J. Sandström, Dynamic NMR Spectroscopy, Academic Press, New York, 1982.
[102] W.J. Grigsby, T. Hascall, J.J. Ellison, M.M. Olmstead, P.P. Power, Inorg. Chem. 35 (1996) 3254.
[103] T. Hascall, K. Ruhlandt-Senge, P.P. Power, Angew. Chem. 106 (1994) 350.
[104] A. Fuchs, E. Kaifer, H.-J. Himmel, Eur. J. Inorg. Chem. (2008) 41.
[105] B. Conway, E. Hevia, A.R. Kennedy, R.E. Mulvey, S. Weatherstone, Dalton Trans. (2005) 1532.
[106] A. Xia, M.J. Heeg, C.H. Winter, Organometallics 21 (2002) 4718.
[107] D.R. Armstrong, W. Clegg, R.E. Mulvey, R.B. Rowlings, J. Chem. Soc., Dalton Trans. (2001) 409.
[108] M. Niemeyer, P.P. Power, Inorg. Chem. 36 (1997) 4688.
[109] M. Gärtner, H. Görls, M. Westerhausen, Organometallics 26 (2007) 1077.
[110] M. Gärtner, H. Görls, M. Westerhausen, J. Organomet. Chem. 693 (2008) 221.
[111] M. Gillett-Kunnath, Thesis Dissertation, Syracuse University, Syracuse, NY 2007.
[112] L. Bourget-Merle, M.F. Lappert, J.R. Severn, Chem. Rev. 102 (2002) 3031.
[113] M.H. Chisholm, J.C. Gallucci, K. Phomphrai, Inorg. Chem. 41 (2002) 2785.
[114] M.H. Chisholm, J.C. Gallucci, K. Phomphrai, Inorg. Chem. 43 (2004) 6717.
[115] C.F. Caro, P.B. Hitchcock, M.F. Lappert, Chem. Commun. (1999) 1433.
[116] H.M. El-Kaderi, A. Xia, M.J. Heeg, C.H. Winter, Organometallics 23 (2004) 3488.
[117] B. Sedal, M.J. Heeg, C.H. Winter, J. Organomet. Chem. 693 (2008) 3495.
[118] H.M. El-Kaderi, M.J. Heeg, C.H. Winter, Organometallics 47 (2004) 4995.
[119] B.M. Chamberlain, M. Cheng, D.R. Moore, T.M. Ovitt, E.B. Lobkovsky, G.W. Coates, J. Am. Chem. Soc. 123 (2001) 3229.
[120] A.G.M. Barrett, M.R. Crimmin, M.S. Hill, G. Kociok-Kohn, J.R. Lachs, P.A. Procopiou, Dalton Trans. (2008) 1292.
[121] A.G.M. Barrett, I.J. Casely, M.R. Crimmin, M.S. Hill, J.R. Lachs, M.F. Mahon, P.A. Procopiou, Inorg. Chem. 48 (2009) 4445.
[122] C. Ruspic, S. Harder, Inorg. Chem. 46 (2007) 10426.
[123] A.P. Dove, V.C. Gibson, P. Hormnirum, E.L. Marshall, J.A. Segal, A.J.P. White, D.J. Williams, Dalton Trans. (2003) 3088.
[124] A.G.M. Barrett, M.R. Crimmin, M.S. Hill, P.B. Hitchcock, P.A. Procopiou, Dalton Trans. (2008) 4474.
[125] R.P. Davies, Inorg. Chem. Commun. 3 (2000) 13.
[126] A.R. Kennedy, R.E. Mulvey, R.B. Rowlings, J. Organomet. Chem. 648 (2002) 288.
[127] L.T. Wendell, J. Bender, X. He, B.C. Noll, K.W. Henderson, Organometallics 25 (2006) 4953.
[128] R.E. Mulvey, Chem. Commun. (2001) 1049.
[129] R.E. Mulvey, Organometallics 25 (2006) 1060.
[130] A. Krasovskiy, B.F. Straub, P. Knochel, Angew. Chem. Int. Ed. 45 (2006) 159.

[131] X. He, J.F. Allan, B.C. Noll, A.R. Kennedy, K.W. Henderson, J. Am. Chem. Soc. 127 (2005) 6920.
[132] X. He, J. Morris, B. Noll, S.N. Brown, K.W. Henderson, J. Am. Chem. Soc. 128 (2006) 13599.
[133] A.R. Kennedy, R.E. Mulvey, R.B. Rowlings, J. Am. Chem. Soc. 120 (1998) 7816.
[134] P.C. Andrikopoulos, D.R. Armstrong, W. Clegg, C.J. Gilfillan, E. Hevia, A.R. Kennedy, R.E. Mulvey, C.T. O'Hara, J.A. Parkinson, D.M. Tooke, J. Am. Chem. Soc. 126 (2004) 11612.
[135] P.C. Andrikopoulos, D.R. Armstrong, A.R. Kennedy, R.E. Mulvey, C.T. O'Hara, R.B. Rowlings, Eur. J. Inorg. Chem. (2003) 3354.
[136] A.M. Drummond, L.T. Gibson, A.R. Kennedy, R.E. Mulvey, C.T. O'Hara, R.B. Rowlings, T. Weightman, Angew. Chem. Int. Ed. 41 (2002) 2382.
[137] G.C. Forbes, F.R. Kenley, A.R. Kennedy, R. Alan, R.E. Mulvey, C.T. O'Hara, J.A. Parkinson, Chem. Commun. (2003) 1140.
[138] D.J. Gallagher, K.W. Henderson, A.R. Kennedy, R. Alan, C.T. O'Hara, R.E. Mulvey, R.B. Rowlings, Chem. Commun. (2002) 376.
[139] E. Hevia, A.R. Kennedy, R.E. Mulvey, S. Weatherstone, Angew. Chem., Int. Ed. 43 (2004) 1709.
[140] A.R. Kennedy, R.E. Mulvey, B.A. Roberts, R.B. Rowlings, C.L. Raston, Chem. Commun. (1999) 353.
[141] P.C. Andrikopoulos, D.R. Armstrong, A.R. Kennedy, R.E. Mulvey, C.T. O'Hara, R.B. Rowlings, S. Weatherstone, Inorg. Chim. Acta 360 (2007) 1370.
[142] X. He, B.C. Noll, A. Beatty, R.E. Mulvey, K.W. Henderson, J. Am. Chem. Soc. 126 (2004) 7444.
[143] A.D. Frankland, P.B. Hitchcock, M.F. Lappert, G.A. Lawless, J. Chem. Soc., Chem. Commun. (1994) 2435.
[144] W. Clegg, K.W. Henderson, R.E. Mulvey, P.A. O'Neil, J. Chem. Soc., Chem. Commun. (1994) 769.
[145] E. Hevia, F.R. Kenley, A.R. Kennedy, R.E. Mulvey, R.B. Rowlings, Eur. J. Inorg. Chem. (2003) 3347.
[146] A. Steiner, D. Stalke, Inorg. Chem. 34 (1995) 4846.
[147] D. Pfeiffer, M.J. Heeg, C.H. Winter, Inorg. Chem. 39 (2000) 2377.
[148] J. Hitzbleck, A.Y. O'Brien, C.M. Forsyth, G.B. Deacon, K. Ruhlandt-Senge, Chem. Eur. J. 10 (2004) 3315.
[149] A.Y. O'Brien, J. Hitzbleck, A. Torvisco, G.B. Deacon, K. Ruhlandt-Senge, Eur. J. Inorg. Chem. (2008) 172.
[150] M.J. Saly, M.J. Heeg, C.H. Winter, Inorg. Chem. 48 (2009) 5303.
[151] J. Hitzbleck, G.B. Deacon, K. Ruhlandt-Senge, Eur. J. Inorg. Chem. (2007) 592.
[152] N.C. Mosch-Zanetti, M. Ferbinteanu, J. Magull, Eur. J. Inorg. Chem. (2002) 950.
[153] J. Hitzbleck, G.B. Deacon, K. Ruhlandt-Senge, Angew. Chem. Int. Ed. 43 (2004) 5218.
[154] J. Hitzbleck, A.Y. O'Brien, G.B. Deacon, K. Ruhlandt-Senge, Inorg. Chem. 45 (2006) 10329.
[155] H.M. El-Kaderi, M.J. Heeg, C.H. Winter, Eur. J. Inorg. Chem. (2005) 2081.
[156] D. Pfeiffer, M.J. Heeg, C.H. Winter, Angew. Chem. Int. Ed. 37 (1998) 2517.
[157] H.M. El-Kaderi, M.J. Heeg, C.H. Winter, Polyhedron 24 (2005) 645.
[158] F. Blanco, I. Alkorta, J. Elguero, J. Phys. Org. Chem. 22 (2009) 747.
[159] H. Schumann, J. Gottfriedsen, J. Demtschuk, Chem. Commun. (1999) 2091.
[160] W. Vargas, K. Ruhlandt-Senge, Eur. J. Inorg. Chem. (2003) 3472.
[161] L.A. Burke, R.N. Butler, J.C. Stephens, J. Chem. Soc., Dalton Trans. (2001) 1679.
[162] F.A. Mautner, C. Gspan, K. Gatterer, M.A.S. Goher, M.A.M. Abu-Youssef, E. Bucher, W. Sitte, Polyhedron 23 (2004) 1217.
[163] T.M. Klapötke, M. Stein, J. Stierstorfer, Z. Anorg. Allg. Chem. 634 (2008) 1711.
[164] I. Kobrsi, J.E. Knox, M.J. Heeg, H.B. Schlegel, C.H. Winter, Inorg. Chem. 44 (2005) 4894.
[165] Y. Guo, G.-H. Tao, Z. Zeng, H. Gao, D.A. Parrish, J.M. Shreeve, Chem. Eur. J. 16 (2010) 3753.
[166] S. Trofimenko, J. Am. Chem. Soc. 89 (1967) 3170.
[167] S. Trofimenko, Scorpionates: The Coordination Chemistry of Polypyrazolylborate Ligands, Imperial College Press, London, 1999.
[168] M.H. Chisholm, Inorg. Chim. Acta 362 (2009) 4284.
[169] A. Garcés, L.F. Sánchez-Barba, C. Alonso-Moreno, M. Fajardo, J. Fernández-Baeza, A. Otero, A. Lara-Sánchez, I. López-Solera, A.M. Rodríguez, Inorg. Chem. 49 (2010) 2859.
[170] E.V. Mutseneck, S. Bieller, M. Bolte, H.-W. Lerner, M. Wagner, Inorg. Chem. 49 (2010) 3540.
[171] J. Zagermann, M.C. Kuchta, K. Merz, N. Metzler-Nolte, Eur. J. Inorg. Chem. (2009) 5407.
[172] D.J. Loroño-Gonzalez, Acta Crystallogr. Sect. A: Found. Crystallogr. C64 (2008) m228.
[173] M.J. Saly, C.H. Winter, Organomet. ASAP (2010).
[174] M.J. Saly, F. Munnik, R.J. Baird, C.H. Winter, Chem. Mater. 21 (2009) 3742.
[175] M.G. Ballinas-López, I.I. Padilla-Martínez, F.J. Martínez-Martínez, H. Höpfl, E.V. García-Báez, Acta Crystallogr. Sect. C: Cryst. Struct. Commun. C62 (2006) m132.
[176] S. Harder, J. Brettar, Angew. Chem. Int. Ed. 45 (2006) 3474.
[177] J.L. Kisko, T. Fillebeen, T. Hascall, G. Parkin, J. Organomet. Chem. 596 (2000) 22.
[178] C. Janiak, S. Temizdemir, T.G. Scharmann, A. Schmalstieg, J. Demtschuk, Z. Anorg. Allg. Chem. 626 (2000) 2053.
[179] C. Pettinari, R. Pettinari, Coord. Chem. Rev. 249 (2005) 525.
[180] H.R. Bigmore, S.C. Lawrence, P. Mountford, C.S. Tredget, Dalton Trans. (2005) 635.
[181] H.R. Bigmore, J. Meyer, I. Krummenacher, H. Ruegger, E. Clot, P. Mountford, F. Breher, Chem. Eur. J. 14 (2008) 5918.
[182] M.G. Cushion, J. Meyer, A. Heath, A.D. Schwarz, I. Fernandez, F. Breher, P. Mountford, Organometallics 29 (2010) 1174.